

# **Potential-based Fracture Mechanics Using Cohesive Zone and Virtual Internal Bond Modeling**

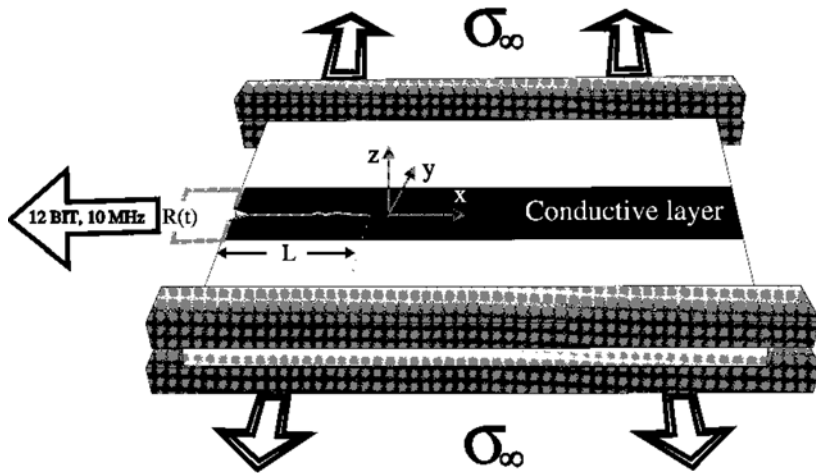
**Kyoungsoo Park**

**7/21/2009**

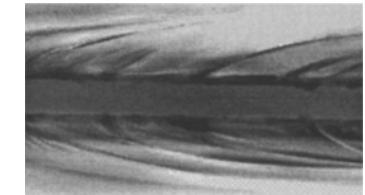
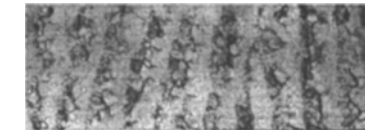
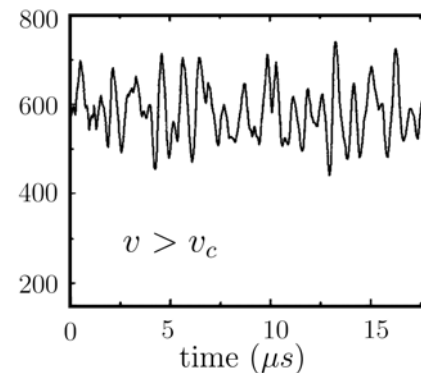
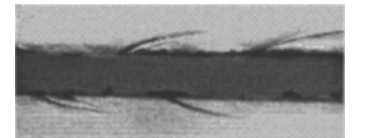
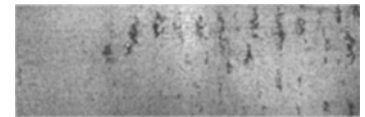
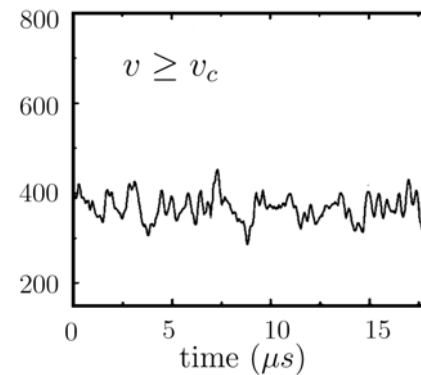
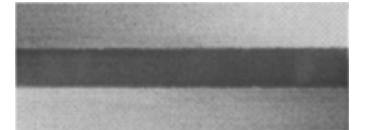
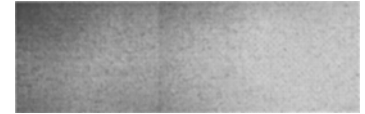
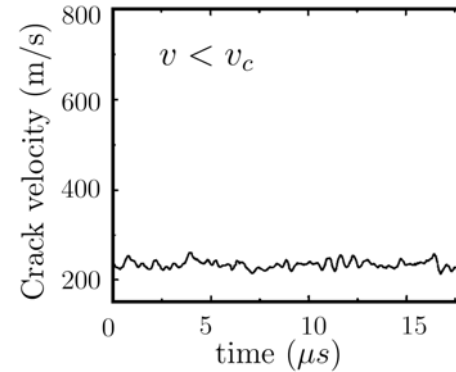
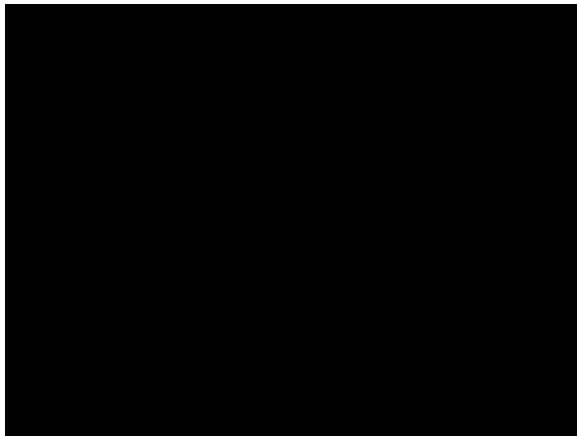
**Advisor/Co-advisor: Glaucio H. Paulino / Jeffery R. Roesler  
Department of Civil & Environmental Engineering  
University of Illinois at Urbana-Champaign**



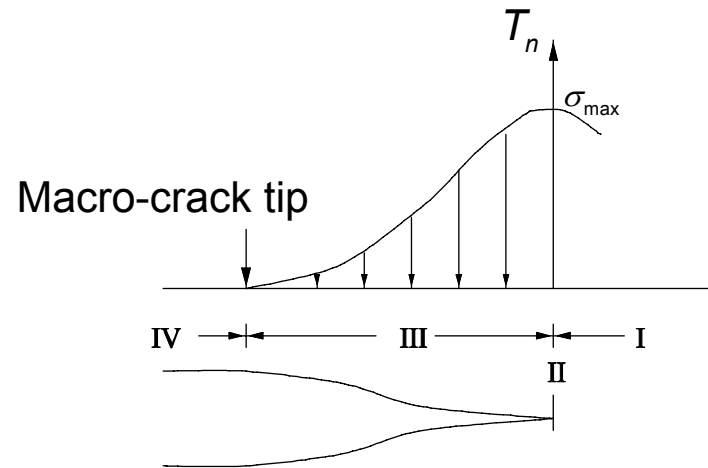
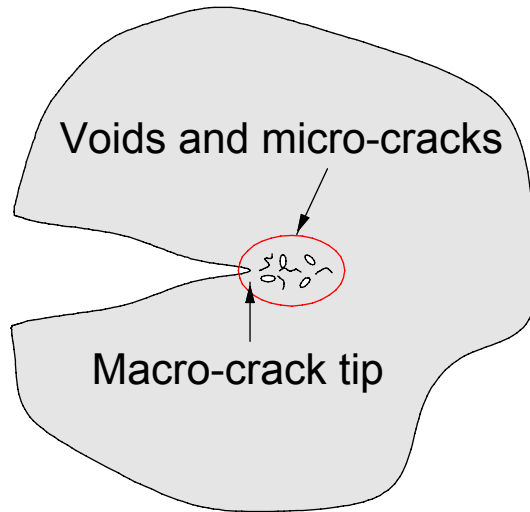
# Micro-Branching Experiment



Sharon E, Fineberg J. Microbranching instability and the dynamic fracture of brittle materials. Physical Review B 1996; 54(10):7128–7139.



# Cohesive Zone Modeling



## □ Constitutive Relationship of Cohesive Fracture

- Non-potential based-model vs. Potential based-model

## □ Computational Methods

- Cohesive surface elements, enrichment functions, embedded discontinuities

- Wells, G. N., Sluys, L. J., 2001. A new method for modelling cohesive cracks using finite elements. *International Journal for Numerical Methods in Engineering* 50 (12), 2667–2682.
- Jirasek, M., 2000. Comparative study on finite elements with embedded discontinuities. *Computer Methods in Applied Mechanics and Engineering* 188 (1-3), 307–330.
- Linder, C., Armero, F., 2009. Finite elements with embedded branching. *Finite Elements in Analysis and Design* 45 (4), 280–293.

# Contents

- Introduction (Ch. 1)
- **Potential-based Cohesive Model (Ch. 3)**
- **Quasi-Static Fracture (Ch. 5)**
  - Particle/matrix debonding
- **Dynamic Fracture Problems (Ch. 4, 6, 7)**
  - Computational framework
  - Micro-branching and fragmentation
  - Mode I predefined crack, mixed-mode and branching
- **Virtual Internal Pair-Bond (VIPB) Model (Ch. 2)**
- **Summary (Ch. 8)**



# Potentials for Cohesive Fracture

- **Needleman, A. (1987)**
    - Polynomial potential / linear shear interaction
  - **Needleman, A. (1990)**
    - Exponential potential / periodic dependence
  - **Beltz, G.E. and Rice, J.R. (1991)**
    - Generalized the potential (Exponential + Sinusoid)
  - **Xu, X.P. and Needleman, A. (1993)**
    - Exponential potential (Exponential + Exponential)
  - **Park, K., Paulino, G.H. and Roesler, J.R. (2009) – PPR**
    - Polynomial potential (Polynomial + Polynomial)
- Needleman A. 1987, A continuum model for void nucleation by inclusion debonding, Journal of Applied Mechanics, 54, 525-531
  - Needleman A. 1990, An analysis of tensile decohesion along an interface, Journal of the Mechanics and Physics of Solid, 3, 289-324
  - Beltz GE and Rice JR, 1991, Dislocation nucleation versus cleavage decohesion at crack tip, Modeling the Deformation of Crystalline Solids, 457-480.
  - Xu XP and Needleman, 1993, Void nucleation by inclusion debonding in a crystal matrix, Modeling Simulation Material Science Engineering, 1, 111-132.
  - Park K, Paulino GH, Roesler JR, 2009, A unified potential-based cohesive model of mixed-mode fracture, Journal of the Mechanics and Physics of Solids 57, 891-908.



# 1. Needleman A. (1987)

Needleman A. 1987, A continuum model for void nucleation by inclusion debonding, Journal of Applied Mechanics, 54, 525-531

## □ Polynomial Potential

$$\Psi(\Delta_n, \Delta_t) = \frac{27}{4} \sigma_{\max} \delta_n \left\{ \frac{1}{2} \left( \frac{\Delta_n}{\delta_n} \right)^2 \left[ 1 - \frac{4}{3} \left( \frac{\Delta_n}{\delta_n} \right) + \frac{1}{2} \left( \frac{\Delta_n}{\delta_n} \right)^2 \right] + \frac{1}{2} \alpha_s \left( \frac{\Delta_t}{\delta_n} \right)^2 \left[ 1 - 2 \left( \frac{\Delta_n}{\delta_n} \right) + \left( \frac{\Delta_n}{\delta_n} \right)^2 \right] \right\}$$

## □ Cohesive Relationship

$$\begin{aligned} \Delta_n \leq \delta_n : \quad T_n &= \frac{\partial \Psi}{\partial \Delta_n} = \frac{27}{4} \sigma_{\max} \left\{ \left( \frac{\Delta_n}{\delta_n} \right) \left[ 1 - 2 \left( \frac{\Delta_n}{\delta_n} \right) + \left( \frac{\Delta_n}{\delta_n} \right)^2 \right] + \alpha_s \left( \frac{\Delta_t}{\delta_n} \right)^2 \left[ \left( \frac{\Delta_n}{\delta_n} \right) - 1 \right] \right\} \\ T_t &= \frac{\partial \Psi}{\partial \Delta_t} = \frac{27}{4} \sigma_{\max} \left\{ \alpha_s \left( \frac{\Delta_t}{\delta_n} \right) \left[ 1 - 2 \left( \frac{\Delta_n}{\delta_n} \right) + \left( \frac{\Delta_n}{\delta_n} \right)^2 \right] \right\} \end{aligned}$$

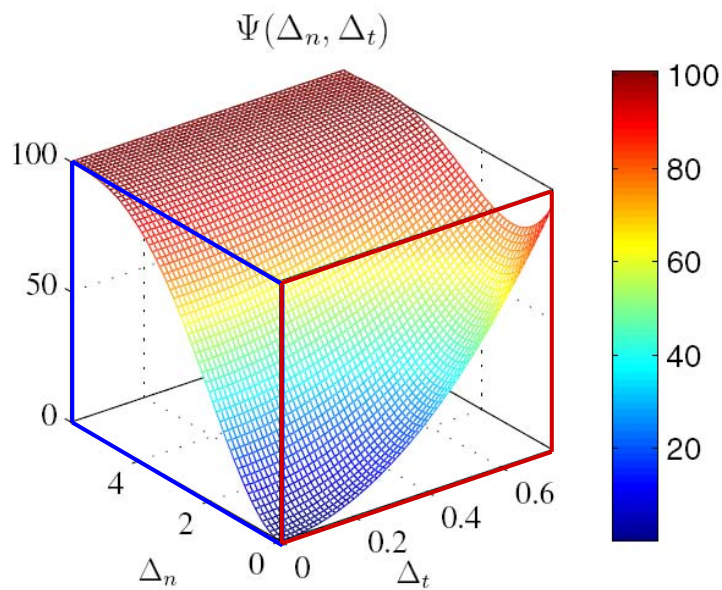
$$\Delta_n > \delta_n : \quad T_n = T_t \equiv 0$$

$$\phi_n = 9 \sigma_{\max} \delta_n / 16$$

$$T_n(0, \delta_n / 3) = \sigma_{\max}$$

**$\alpha_s$ : shear stiffness parameter**  
**Shear dependence  $\rightarrow$  linear**  
**Displacement jump  $\rightarrow$  small**





$$T_n = \frac{27}{4} \sigma_{\max} \left\{ \left( \frac{\Delta_n}{\delta_n} \right) \left[ 1 - 2 \left( \frac{\Delta_n}{\delta_n} \right) + \left( \frac{\Delta_n}{\delta_n} \right)^2 \right] + \alpha_s \left( \frac{\Delta_t}{\delta_n} \right)^2 \left[ \left( \frac{\Delta_n}{\delta_n} \right) - 1 \right] \right\}$$

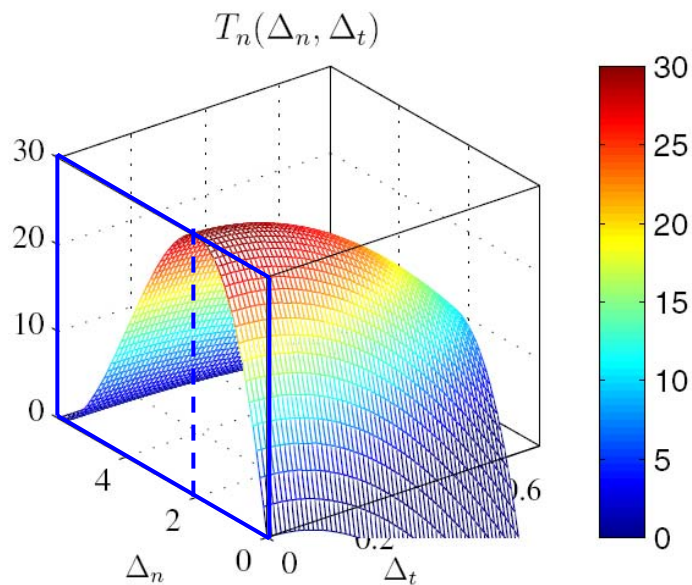
$$T_t = \frac{27}{4} \sigma_{\max} \left\{ \alpha_s \left( \frac{\Delta_t}{\delta_n} \right) \left[ 1 - 2 \left( \frac{\Delta_n}{\delta_n} \right) + \left( \frac{\Delta_n}{\delta_n} \right)^2 \right] \right\}$$

$$\phi_n = 100 \text{ N/m}$$

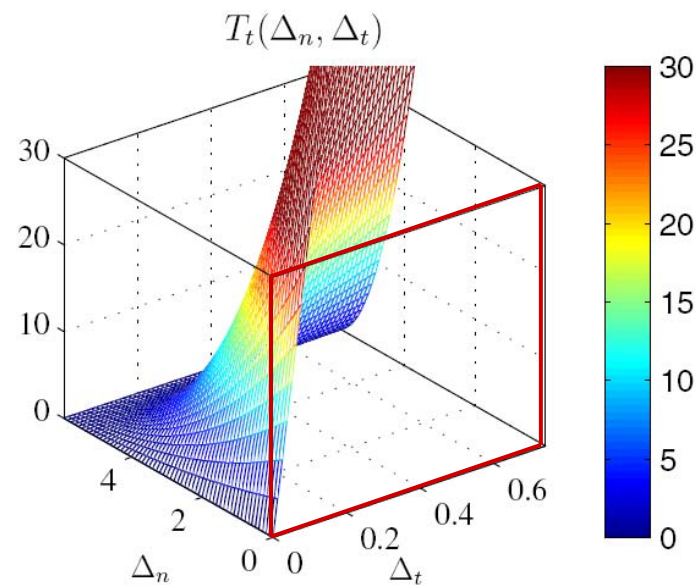
$$\sigma_{\max} = 30 \text{ MPa}$$

$$\alpha_s = 10$$

Axis	Units
$\Psi$	N/m
$T_n, T_t$	MPa
$\Delta_n, \Delta_t$	$\mu\text{m}$



**Mode I**



**Mode II**

# 2. Needleman A. (1990)

Needleman A. 1990, An analysis of tensile decohesion along an interface, Journal of the Mechanics and Physics of Solid, 3, 289-324

## □ Exponential Potential with Periodic Dependence

$$\Psi(\Delta_n, \Delta_t) = \frac{\sigma_{\max} e^{\delta_n}}{z} \left\{ 1 - \left[ 1 + \frac{z\Delta_n}{\delta_n} - \beta_s z^2 \left[ 1 - \cos\left(\frac{2\pi\Delta_t}{\delta_t}\right) \right] \right] \exp\left(-\frac{z\Delta_n}{\delta_n}\right) \right\}$$

## □ Motivation

### ■ Universal binding energy (Normal direction)

$$E(a) = -(1 + \beta a) \exp(-\beta a)$$

Rose JH, Rerrante J and Smith JR, 1981, Universal binding energy curves for metals and bimetallic interfaces, Physical Review Letters, 47, 675-678

### ■ Periodicity of the underlying lattice (Tangential direction)

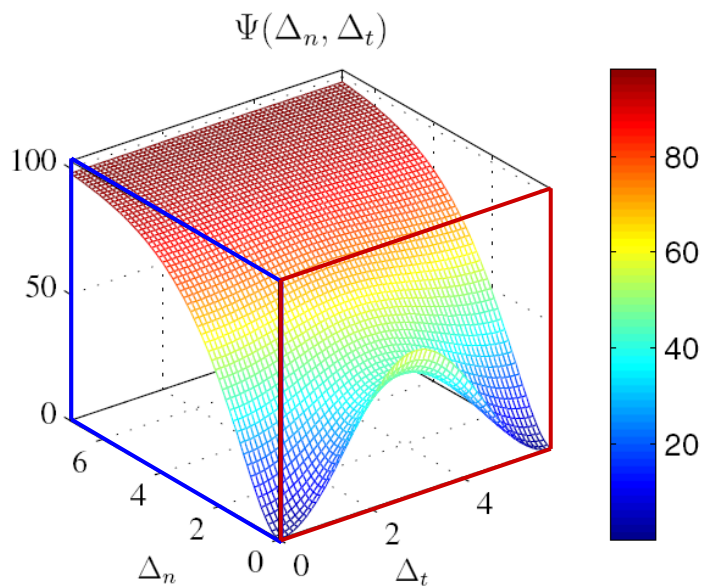
## □ Cohesive Relationship

$$T_n = \sigma_{\max} e^{\left\{ \frac{z\Delta_n}{\delta_n} - \beta_s z^2 \left[ 1 - \cos\left(\frac{2\pi\Delta_t}{\delta_t}\right) \right] \right\}} \exp\left(-\frac{z\Delta_n}{\delta_n}\right)$$

$$T_t = \sigma_{\max} e^{\left\{ 2\pi\beta_s z \left(\frac{\delta_n}{\delta_t}\right) \sin\left(\frac{2\pi\Delta_t}{\delta_t}\right) \right\}} \exp\left(-\frac{z\Delta_n}{\delta_n}\right)$$







$$T_n = \sigma_{\max} e^{\left\{ \frac{z\Delta_n}{\delta_n} - \beta_s z^2 \left[ 1 - \cos\left(\frac{2\pi\Delta_t}{\delta_t}\right) \right] \right\}} \exp\left(-\frac{z\Delta_n}{\delta_n}\right)$$

$$T_t = \sigma_{\max} e^{\left\{ 2\pi\beta_s z \left(\frac{\delta_n}{\delta_t}\right) \sin\left(\frac{2\pi\Delta_t}{\delta_t}\right) \right\}} \exp\left(-\frac{z\Delta_n}{\delta_n}\right)$$

$$\phi_n = 100 \text{ N/m}$$

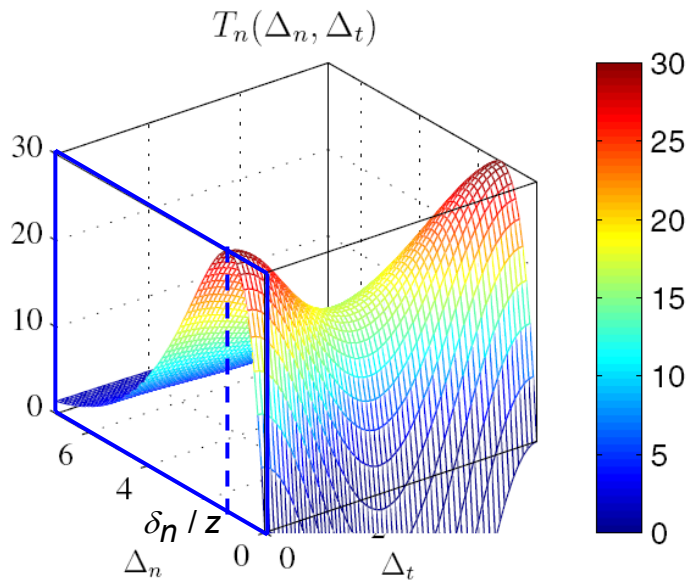
$$\sigma_{\max} = 30 \text{ MPa}$$

$$z = 16e/9$$

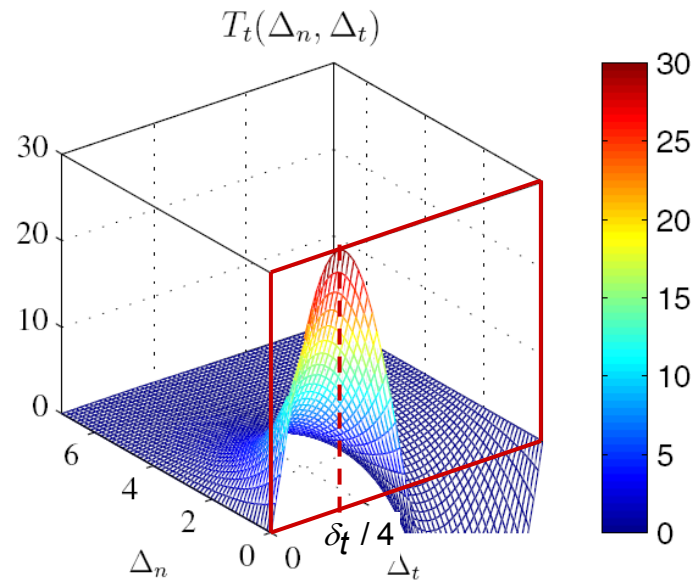
$$\delta_n = \frac{z\phi_n}{e\sigma_{\max}}$$

$$\delta_n = \delta_t$$

$$\beta_s = 1/2\pi ez$$



**Mode I**



**Mode II**

# 3. Beltz G.E. and Rice J.R. (1991)

Beltz GE and Rice JR, 1991, Dislocation nucleation versus cleavage decohesion at crack tip, Modeling the Deformation of Crystalline Solids, 457-480.

## □ Cohesive Relationship

- Normal direction: Exponential  $\rightarrow T_n = [B(\Delta_t)\Delta_n - C(\Delta_t)] \exp(-\Delta_n/\delta_n)$
- Tangential direction: Sinusoid  $\rightarrow T_t = A(\Delta_n) \sin\left(\frac{2\pi\Delta_t}{\delta_t}\right)$
- Boundary Condition + Exact differential (Potential)  $\frac{\partial T_n}{\partial \Delta_t} = \frac{\partial T_t}{\partial \Delta_n}$

$$\int_0^\infty T_n(\Delta_n, 0) d\Delta_n = 2\gamma_s = \phi_n$$

$$\int_0^{\delta_t/2} T_t(0, \Delta_t) d\Delta_t = \gamma_{us} = \phi_t$$

$$C(0) = 0$$

$$T_n = \frac{\phi_n}{\delta_n^2} \Delta_n \exp\left(-\frac{\Delta_n}{\delta_n}\right)$$

Universal bonding correlation.

$$\lim_{\Delta_n \rightarrow \infty} T_n(\Delta_n, \Delta_t) = 0$$

$$\lim_{\Delta_n \rightarrow \infty} T_t(\Delta_n, \Delta_t) = 0$$

$$\lim_{\Delta_t \rightarrow b/2} T_t(\Delta_n, \Delta_t) = 0$$

$$\lim_{\Delta_t \rightarrow b/2} T_n(\Delta_n, \Delta_t) \neq 0$$

Rose JH, Rerrante J and Smith JR, 1981, Universal binding energy curves for metals and bimetallic interfaces, *Physical Review Letters*, 47, 675-678

Introduce additional condition  $\Delta_n^*$  instead of  $\lim_{\Delta_t \rightarrow b/2} T_n(\Delta_n, \Delta_t) = 0$

$$T_n(\Delta_n^*, b/2) = [B(b/2)\Delta_n^* - C(b/2)] e^{-\Delta_n^*/\delta_n} = 0$$



# 3. Beltz G.E. and Rice J.R. (1991)

## □ Solve PDE with BCs

$$\frac{\partial T_n}{\partial \Delta_t} = \frac{\partial T_t}{\partial \Delta_n}$$

$$T_n = [B(\Delta_t)\Delta_n - C(\Delta_t)] \exp(-\Delta_n/\delta_n)$$

$$T_t = A(\Delta_n) \sin\left(\frac{2\pi\Delta_t}{\delta_t}\right)$$

$$\int_0^\infty T_n(\Delta_n, 0) d\Delta_n = 2\gamma_s = \phi_n$$

$$\int_0^{\delta_t/2} T_t(0, \Delta_t) d\Delta_t = \gamma_{us} = \phi_t$$

$$\lim_{\Delta_n \rightarrow \infty} T_n(\Delta_n, \Delta_t) = 0 \quad \lim_{\Delta_n \rightarrow \infty} T_t(\Delta_n, \Delta_t) = 0$$

$$C(0) = 0$$

$$A(\Delta_n) = \frac{\pi\gamma_{us}}{\delta_t} - \frac{2\pi\gamma_s}{\delta_t} \left\{ q \left[ 1 - \exp\left(-\frac{\Delta_n}{\delta_n}\right) \right] - \left(\frac{q-r}{1-r}\right) \frac{\Delta_n}{\delta_n} \exp\left(-\frac{\Delta_n}{\delta_n}\right) \right\} \quad q = \frac{\gamma_{us}}{2\gamma_s}$$

$$B(\Delta_t) = \frac{2\gamma_s}{\delta_n^2} \left\{ 1 - \left(\frac{q-r}{1-r}\right) \sin^2\left(\frac{2\pi\Delta_t}{\delta_t}\right) \right\} \quad r = \frac{\Delta_n^*}{\delta_n}$$

$$C(\Delta_t) = \frac{2\gamma_s}{\delta_n} \frac{r(1-q)}{1-r} \sin^2\left(\frac{2\pi\Delta_t}{\delta_t}\right)$$

$$\Psi = 2\gamma_s + 2\gamma_s \exp\left(-\frac{\Delta_n}{\delta_n}\right) \left\{ \left[ q + \left(\frac{q-r}{1-r}\right) \frac{\Delta_n}{\delta_n} \right] \sin^2\left(\frac{2\pi\Delta_t}{\delta_t}\right) - \left[ 1 + \frac{\Delta_n}{\delta_n} \right] \right\}$$

$$E(a) = -(1 + \beta a) \exp(-\beta a)$$

Rose JH, Rerrante J and Smith JR, 1981, Universal binding energy curves for metals and bimetallic interfaces, *Physical Review Letters*, 47, 675-678



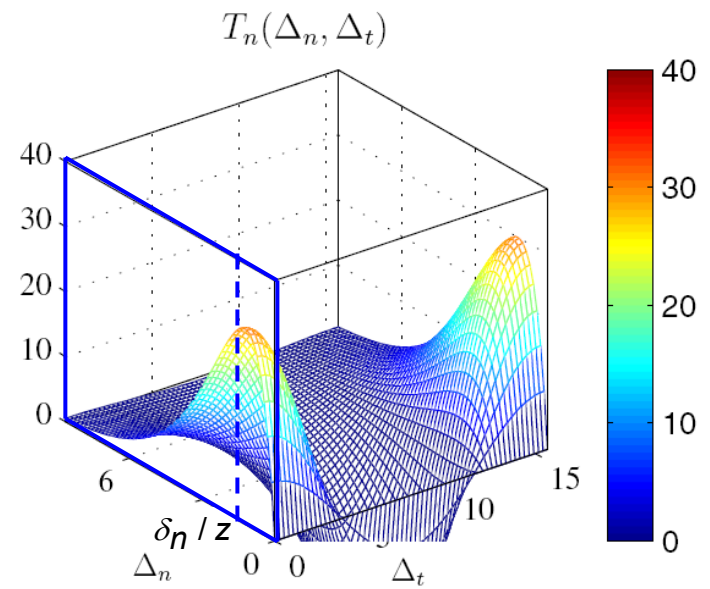
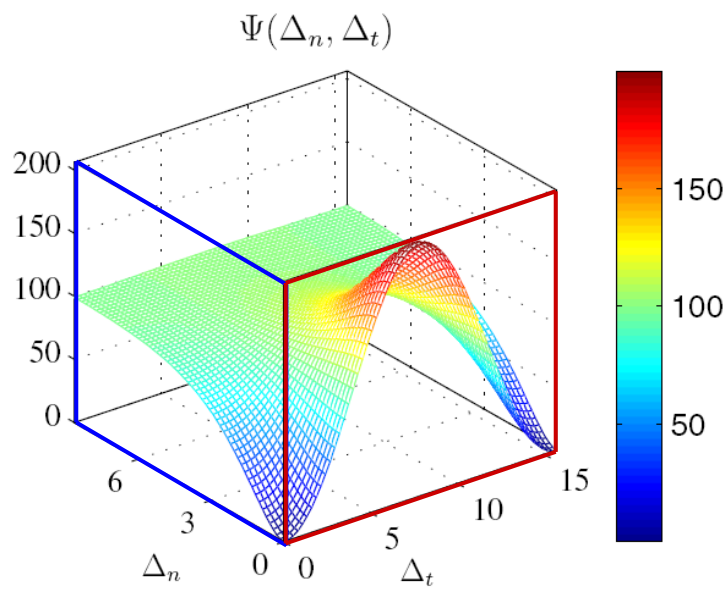
$$\phi_n = 100 \text{ N/m} \quad \sigma_{\max} = 30 \text{ MPa}$$

$$\phi_t = 200 \text{ N/m} \quad \tau_{\max} = 40 \text{ MPa}$$

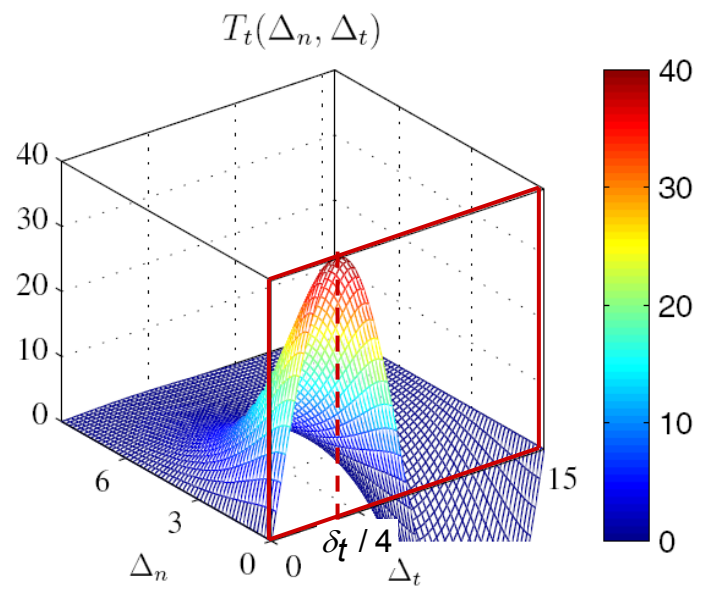
$$r = \frac{\Delta_n^*}{\delta_n} = 0$$

“ $\Delta_n^*$  is the value of  $\Delta_n$  after shearing to the state  $\Delta_t = b/2$  under conditions of zero tension,  $T_n = 0$  (i.e. relaxed shearing)”

$$T_n(\Delta_n^*, b/2) = [B(b/2)\Delta_n^* - C(b/2)]e^{-\Delta_n^*/\delta_n} = 0$$



**Mode I**



**Mode II**

# 4. Xu X.P. and Needleman A. (1993)

Xu XP and Needleman, 1993, Void nucleation by inclusion debonding in a crystal matrix, Modeling Simulation Material Science Engineering, 1, 111-132.

## □ Cohesive Relationship

- Normal direction: Exponential  $\rightarrow T_n = [B(\Delta_t)\Delta_n - C(\Delta_t)]\exp(-\Delta_n / \delta_n)$
- Tangential direction: Exponential  $\rightarrow T_t = A(\Delta_n) \frac{\Delta_t}{\delta_t} \exp(-\Delta_t^2 / \delta_t^2)$
- Boundary Condition

$$\phi_n = \int_0^\infty T_n(\Delta_n, 0) d\Delta_n \quad \phi_t = \int_0^\infty T_t(0, \Delta_t) d\Delta_t \quad C(0) = 0$$

$$\lim_{\Delta n \rightarrow \infty} T_n(\Delta_n, \Delta_t) = 0$$

$$\lim_{\Delta n \rightarrow \infty} T_t(\Delta_n, \Delta_t) = 0$$

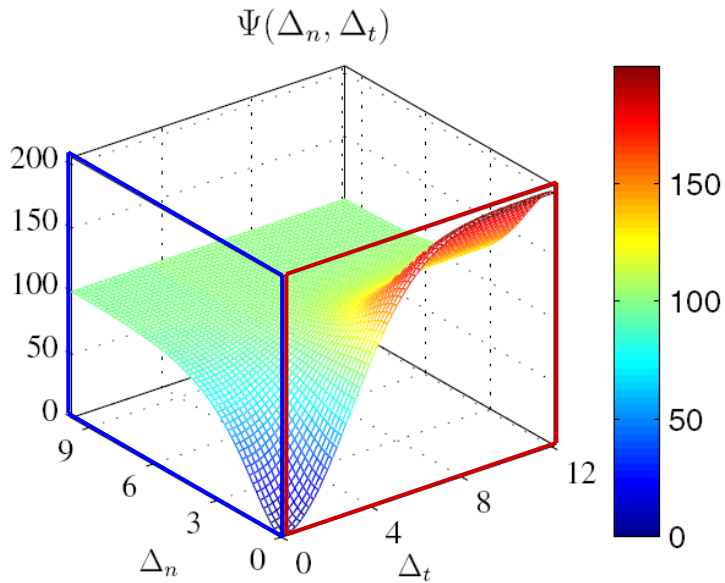
$$\lim_{\Delta n \rightarrow \infty} T_t(\Delta_n, \Delta_t) = 0$$

$$\lim_{\Delta t \rightarrow \infty} T_n(\Delta_n, \Delta_t) \neq 0$$

Introduce additional condition  $\Delta_n^*$  instead of  $\lim_{\Delta t \rightarrow \infty} T_n(\Delta_n, \Delta_t) = 0$

$$\lim_{\Delta t \rightarrow \infty} T_n(\Delta_n^*, \Delta_t) = 0$$

$$\Psi(\Delta_n, \Delta_t) = \phi_n + \phi_n \exp\left(\frac{-\Delta_n}{\delta_n}\right) \left\{ \left[ 1 - r + \frac{\Delta_n}{\delta_n} \right] \frac{(1-q)}{(r-1)} - \left[ q + \frac{(r-q)\Delta_n}{(r-1)\delta_n} \right] \exp\left(-\frac{\Delta_t^2}{\delta_t^2}\right) \right\}$$



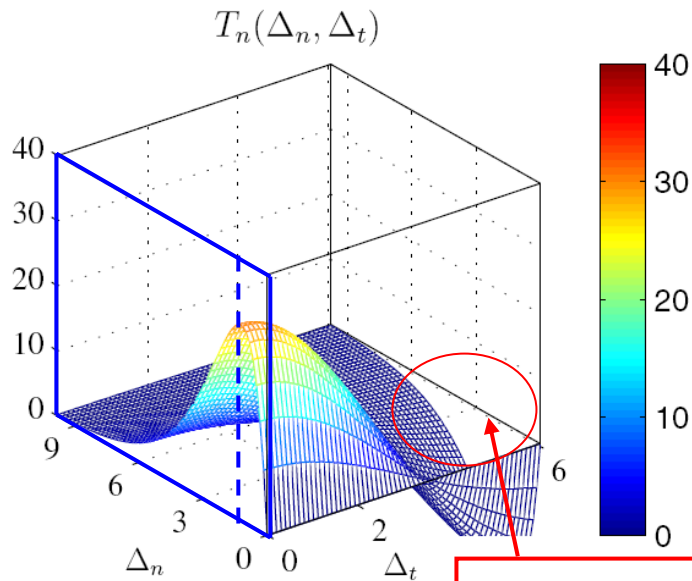
$$\phi_n = 100 \text{ N/m}$$

$$\phi_t = 200 \text{ N/m}$$

$$\sigma_{\max} = 30 \text{ MPa}$$

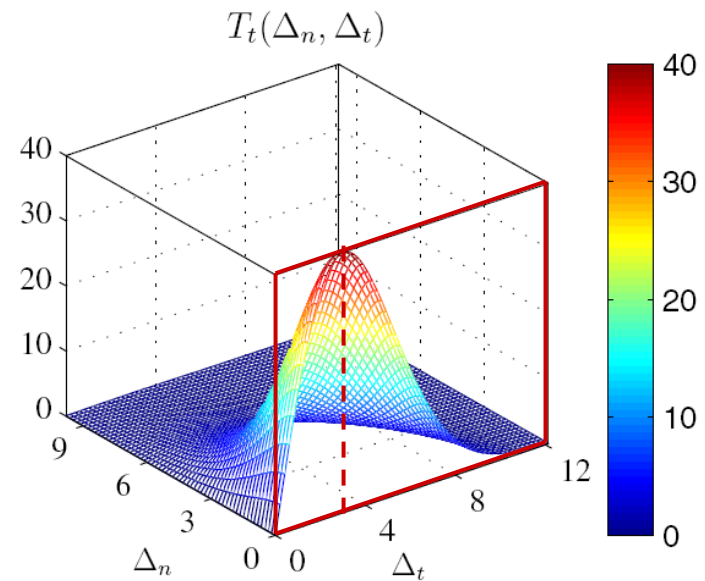
$$\tau_{\max} = 40 \text{ MPa}$$

$$r = \frac{\Delta_n^*}{\delta_n} = 0$$



**Mode I**

$$\lim_{\Delta_t \rightarrow \infty} T_n(\Delta_n, \Delta_t) < 0$$



**Mode II**



# Remarks

## □ Previous Potential

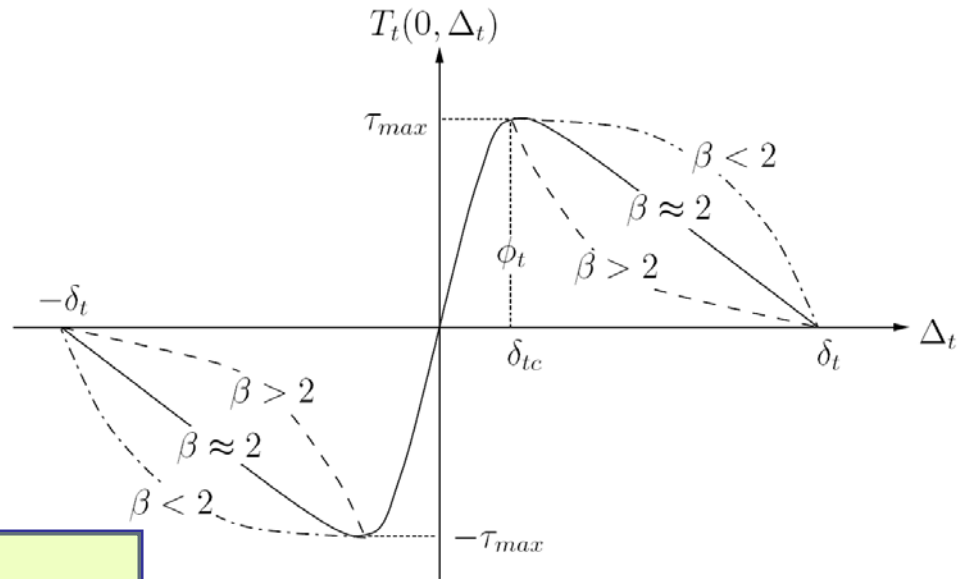
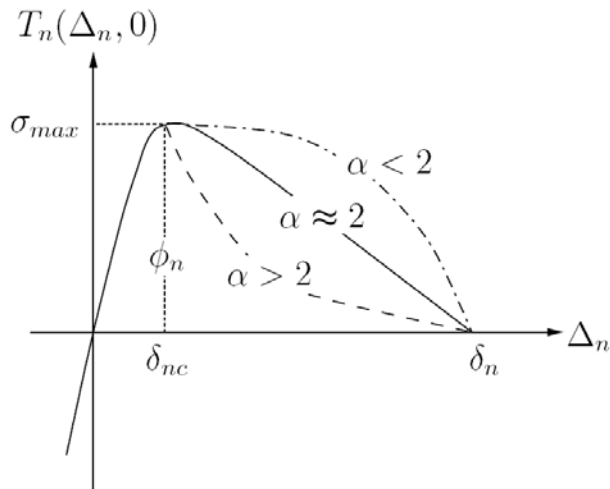
- Boundary condition is not symmetric  $\rightarrow \lim_{\Delta t \rightarrow \infty} T_n(\Delta_n, \Delta_t) \neq 0$
- Vague fracture parameter,  $r$  (or  $\Delta_n^*$ )  $\rightarrow$  Okay if fracture energies are the same
- Complete separation at infinity
- Could not control initial slope  $\rightarrow$  Large compliance

## □ Proposed Potential

- Expressed by a single function
- Different fracture energy :  $\phi_n, \phi_t$
- Different cohesive strength :  $\sigma_{\max}, \tau_{\max}$
- Different cohesive law:  $\alpha, \beta$
- Different initial slope :  $\lambda_n, \lambda_t$



# Boundary Conditions



$$\phi_n = \int_0^{\delta_n} T_n(\Delta_n, 0) d\Delta_n$$

$$\left. \frac{\partial T_n}{\partial \Delta_n} \right|_{\Delta_n = \delta_{nc}} = 0$$

$$T_n(\delta_{nc}, 0) = \sigma_{max}$$

$$T_n(\delta_n, \Delta_t) = 0$$

$$T_n(\Delta_n, \bar{\delta}_t) = 0$$

$$\phi_t = \int_0^{\delta_t} T_t(0, \Delta_t) d\Delta_t$$

$$\left. \frac{\partial T_t}{\partial \Delta_t} \right|_{\Delta_t = \delta_{tc}} = 0$$

$$T_t(0, \delta_{tc}) = \tau_{max}$$

$$T_t(\Delta_n, \delta_t) = 0$$

$$T_t(\bar{\delta}_n, \Delta_t) = 0$$

**Various material behavior, i.e.**

**Plateau-type**  $1 < \alpha, \beta \ll 2$

**Brittle material**  $\alpha, \beta \approx 2$

**Quasi-brittle material**  $\alpha, \beta \gg 2$



# PPR: Unified Mixed Mode Potential

$$\Psi(\Delta_n, \Delta_t) = \min(\phi_n, \phi_t) + \left[ \Gamma_n \left(1 - \frac{\Delta_n}{\delta_n}\right)^\alpha \left(\frac{m}{\alpha} + \frac{\Delta_n}{\delta_n}\right)^m + \langle \phi_n - \phi_t \rangle \right] \left[ \Gamma_t \left(1 - \frac{|\Delta_t|}{\delta_t}\right)^\beta \left(\frac{n}{\beta} + \frac{|\Delta_t|}{\delta_t}\right)^n + \langle \phi_t - \phi_n \rangle \right]$$

□ **Energy Constants:**  $\sqrt[n]{\Gamma_n}$  and  $\sqrt[t]{\Gamma_t}$

□ **Exponents:**  $m$  and  $n$

□ **Characteristic length scales:**  $\delta_n$  and  $\delta_t$

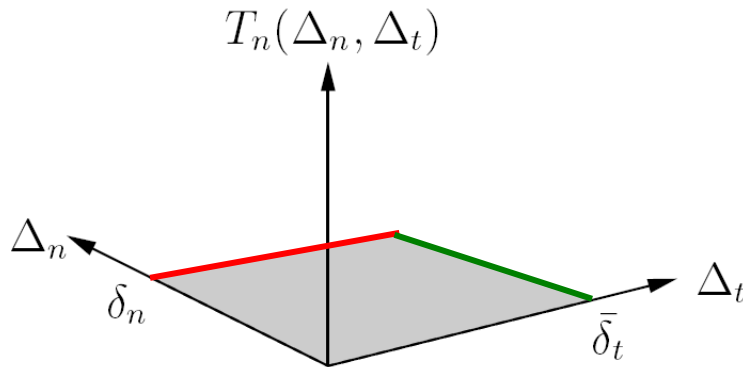
□ **Shape parameters :**  $\alpha$  and  $\beta$

- **Fracture energy**
- **Cohesive strength**
- **Cohesive interaction shape**
- **Initial slope**

K. Park, GH. Paulino, JR. Roesler, 2009, A unified potential-based cohesive model of mixed-mode fracture, *Journal of the Mechanics and Physics of Solids* 57, 891-908.



# Softening Region

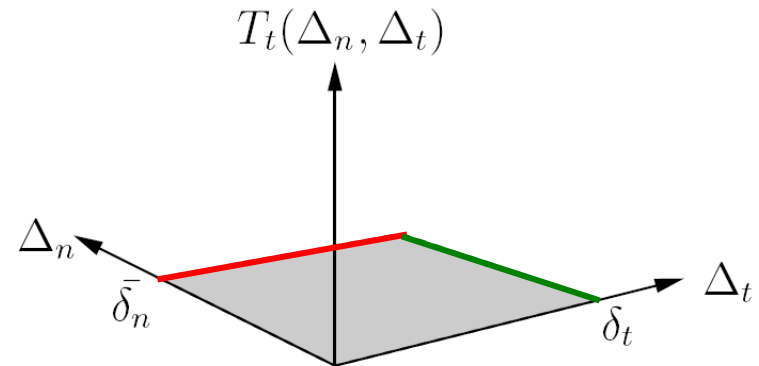


$$T_n(\delta_n, \Delta_t) = 0$$

$$\delta_n = \frac{\phi_n}{\sigma_{\max}} \alpha \lambda_n (1 - \lambda_n)^{\alpha-1} \left( \frac{\alpha}{m} + 1 \right) \left( \frac{\alpha}{m} \lambda_n + 1 \right)^{m-1}$$

$$T_n(\Delta_n, \bar{\delta}_t) = 0$$

$$f_t(\Delta_t) = \Gamma_t \left( 1 - \frac{|\Delta_t|}{\delta_t} \right)^\beta \left( \frac{n}{\beta} + \frac{|\Delta_t|}{\delta_t} \right)^n + \langle \phi_t - \phi_n \rangle = 0$$



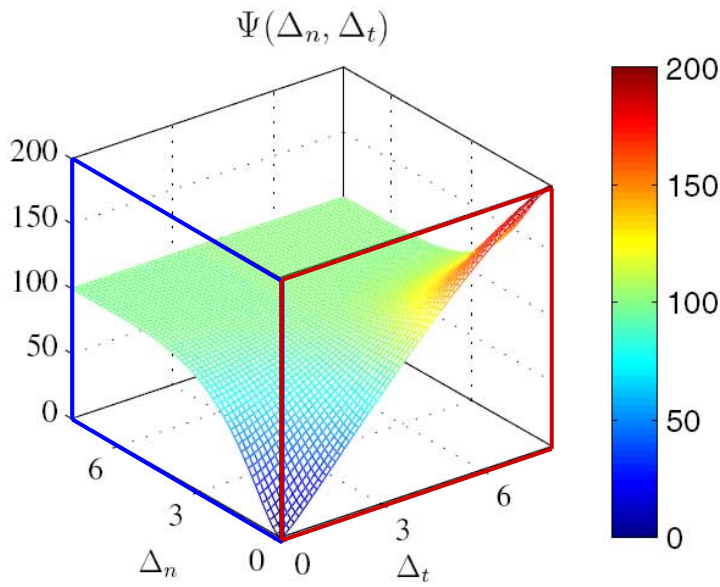
$$T_t(\bar{\delta}_n, \Delta_t) = 0$$

$$f_n(\Delta_n) = \Gamma_n \left( 1 - \frac{\Delta_n}{\bar{\delta}_n} \right)^\alpha \left( \frac{m}{\alpha} + \frac{\Delta_n}{\bar{\delta}_n} \right)^m + \langle \phi_n - \phi_t \rangle = 0$$

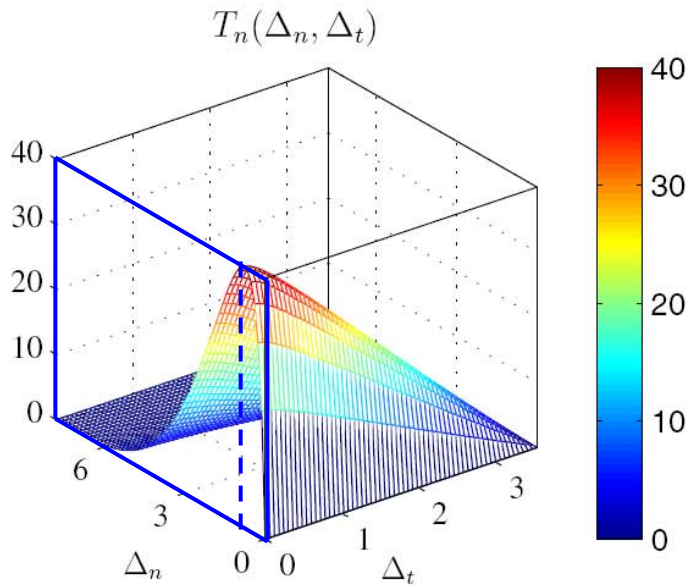
$$T_t(\Delta_n, \delta_t) = 0$$

$$\delta_t = \frac{\phi_t}{\tau_{\max}} \beta \lambda_t (1 - \lambda_t)^{\beta-1} \left( \frac{\beta}{n} + 1 \right) \left( \frac{\beta}{n} \lambda_t + 1 \right)^{n-1}$$

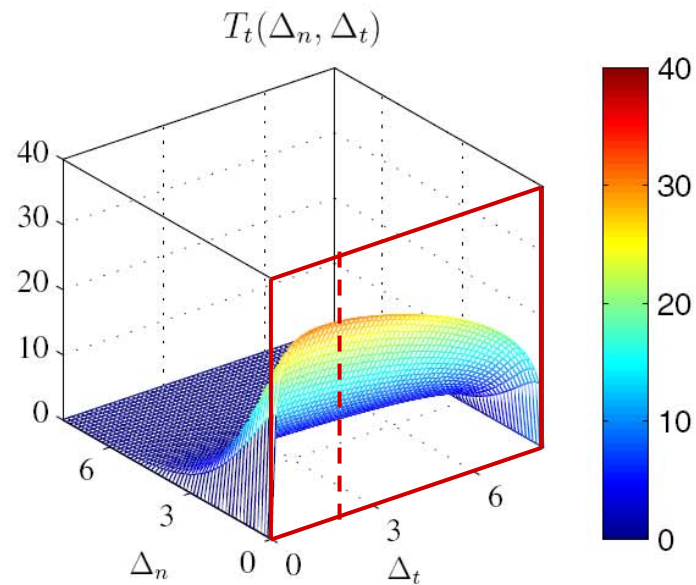
- Fracture energy
- Cohesive strength
- Cohesive interaction shape
- Initial slope



$\phi_n = 100 \text{ N / m}$	$\phi_t = 200 \text{ N / m}$
$\sigma_{\max} = 40 \text{ MPa}$	$\tau_{\max} = 30 \text{ MPa}$
$\alpha = 5$	$\beta = 1.3$
$\lambda_n = 0.1$	$\lambda_t = 0.2$



**Mode I**



**Mode II**

# Extension for the **EXTRINSIC** Model

## □ Correct Limit Procedure

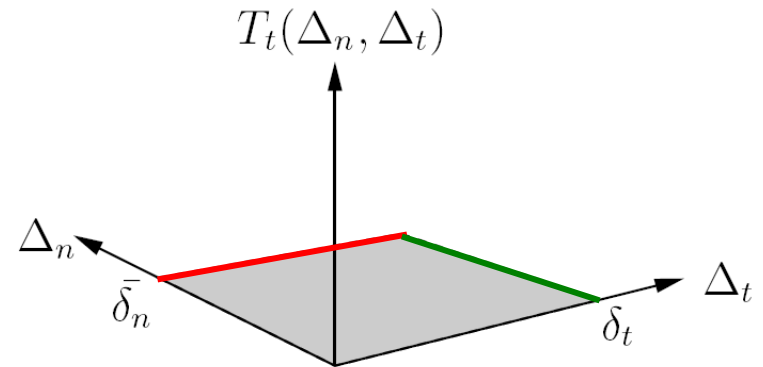
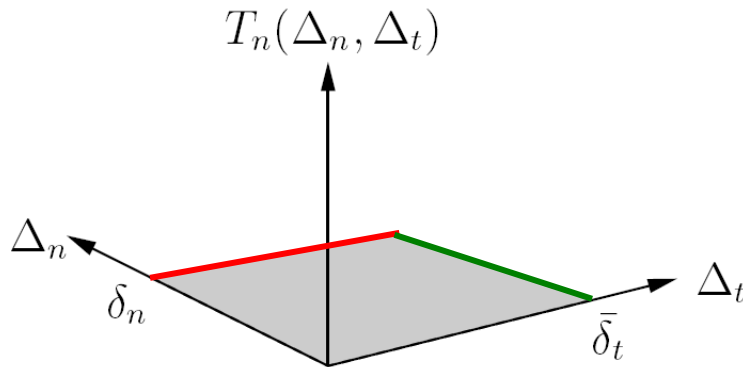
- Limit of initial slope indicators in the potential

$$\Psi(\Delta_n, \Delta_t) = \min(\phi_n, \phi_t) + \left[ \Gamma_n \left( 1 - \frac{\Delta_n}{\delta_n} \right)^\alpha + \langle \phi_n - \phi_t \rangle \right] \left[ \Gamma_t \left( 1 - \frac{|\Delta_t|}{\delta_t} \right)^\beta + \langle \phi_t - \phi_n \rangle \right]$$

- Energy constants:  $\sqrt{\Gamma_n}$  and  $\sqrt{\Gamma_t}$
  - Characteristic length scales:  $\delta_n$  and  $\delta_t$
  - Shape parameters:  $\alpha$  and  $\beta$
- Exclude elastic behavior → **Extrinsic model**
- Consider different fracture energy:  $\phi_n, \phi_t$
- Describe different cohesive strength:  $\sigma_{\max}, \tau_{\max}$
- Represent various cohesive shape:  $\alpha, \beta$



# Softening Region



$$T_n(\delta_n, \Delta_t) = 0$$

$$\delta_n = \alpha \phi_n / \sigma_{\max}$$

$$T_n(\Delta_n, \bar{\delta}_t) = 0$$

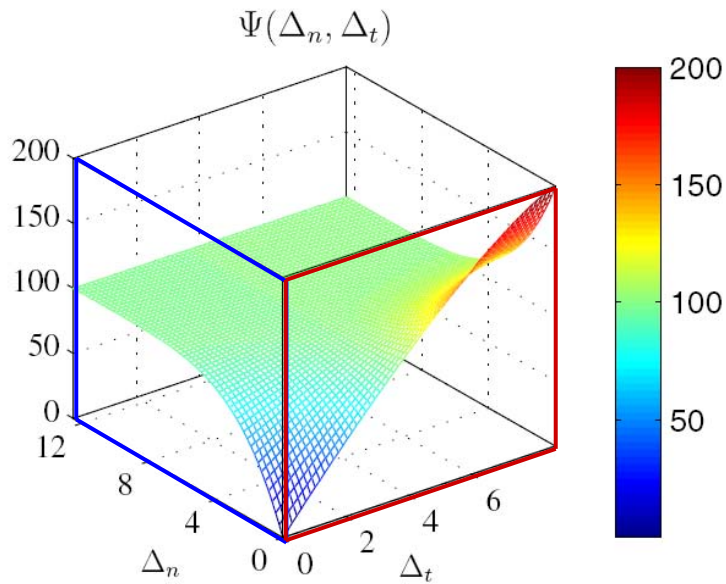
$$\bar{\delta}_t = \delta_t - \delta_t \left( \frac{\langle \phi_t - \phi_n \rangle}{\phi_t} \right)^{1/\beta}$$

$$T_t(\bar{\delta}_n, \Delta_t) = 0$$

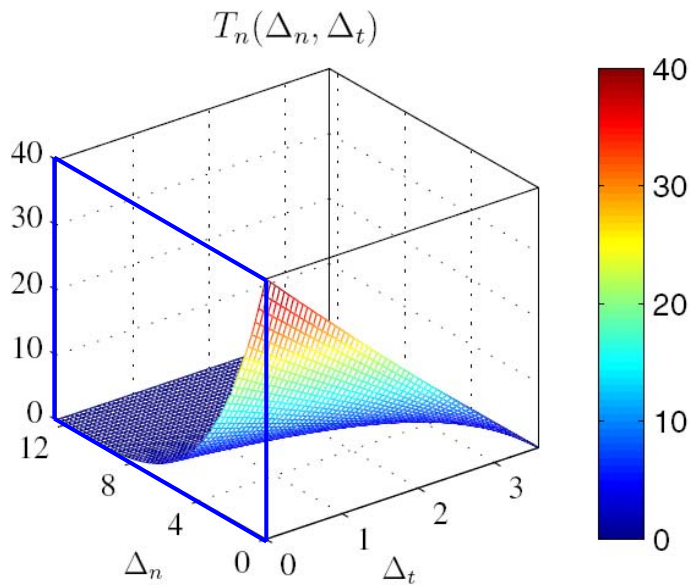
$$\bar{\delta}_n = \delta_n - \delta_n \left( \frac{\langle \phi_n - \phi_t \rangle}{\phi_n} \right)^{1/\alpha}$$

$$T_t(\Delta_n, \delta_t) = 0$$

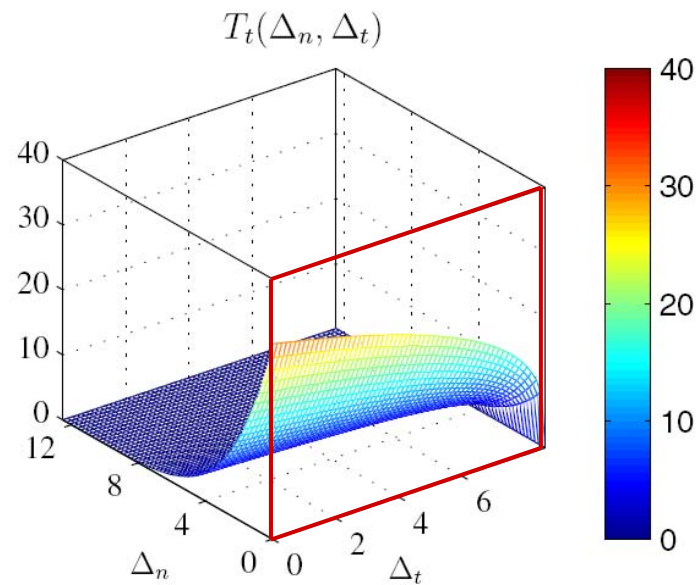
$$\delta_t = \beta \phi_t / \tau_{\max}$$



$\phi_n = 100 \text{ N/m}$	$\phi_t = 200 \text{ N/m}$
$\sigma_{\max} = 40 \text{ MPa}$	$\tau_{\max} = 30 \text{ MPa}$
$\alpha = 5$	$\beta = 1.3$



**Mode I**



**Mode II**

# Remarks

- **Consistent boundary condition**
- **Fracture parameters**
  - Energy, strength, shape, slope
- **Intrinsic/Extrinsic cohesive zone modeling**
- **Path dependence of work-of-separation**
  - Proportional path
  - Non-proportional path
- **Unloading/reloading relationship is independent of the potential-based model**
  - Coupled unloading/reloading relationship
  - Uncoupled unloading/reloading relationship



# Contents

- Introduction
- Potential-based Cohesive Model
- **Quasi-Static Fracture**
  - Particle/matrix debonding
- **Dynamic Fracture Problems**
  - Computational framework
  - Micro-branching and fragmentation
  - Mode I predefined crack, mixed-mode and branching
- **Virtual Internal Pair-Bond (VIPB) Model**
- **Summary**





# Particle/Matrix Debonding

## □ Macroscopic Constitutive Relationship

## □ Micromechanics

### ■ Extended Mori-Tanaka Method

#### □ Hydro-static state

#### □ Interface debonding of cohesive constitutive relationship

Tan, H., Huang, Y., Liu, C., Ravichandran, G., Paulino, G. H., 2007. Constitutive behaviors of composites with interface debonding: The extended Mori-Tanaka method for uniaxial tension. *International Journal of Fracture* 146 (3), 139–148.

## □ Computational Method

### ■ Cohesive surface elements

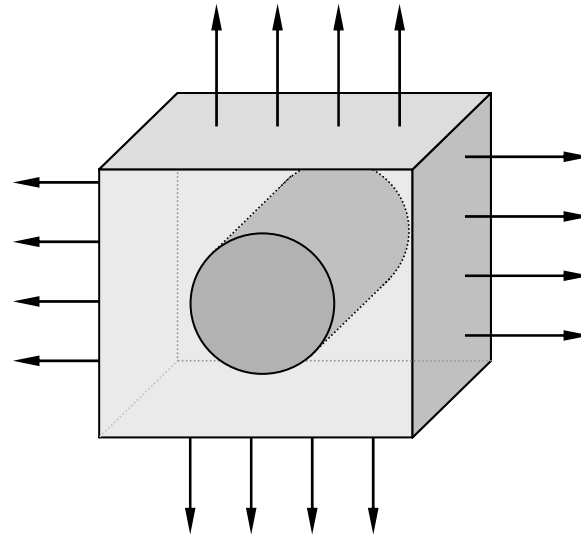


# Finite Element Analysis

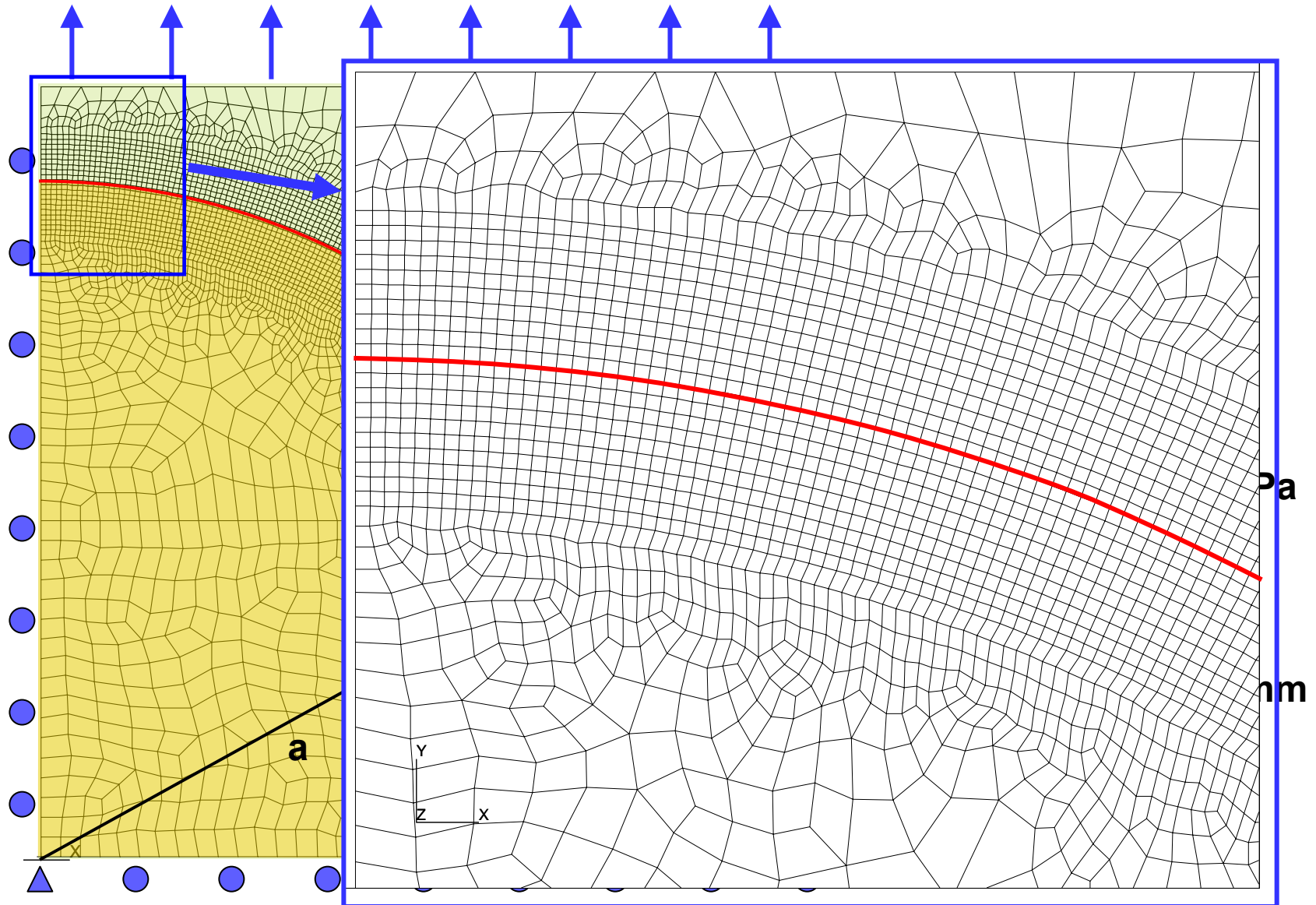
## □ Equi-biaxial Tension

## □ Assumptions

- Reduced to 2D Problem
  - Plane strain
- Quarter domain
  - Symmetry boundary conditions of unit cell
- Poisson's ratio = 0.25
- Cohesive surface elements are inserted along the interface

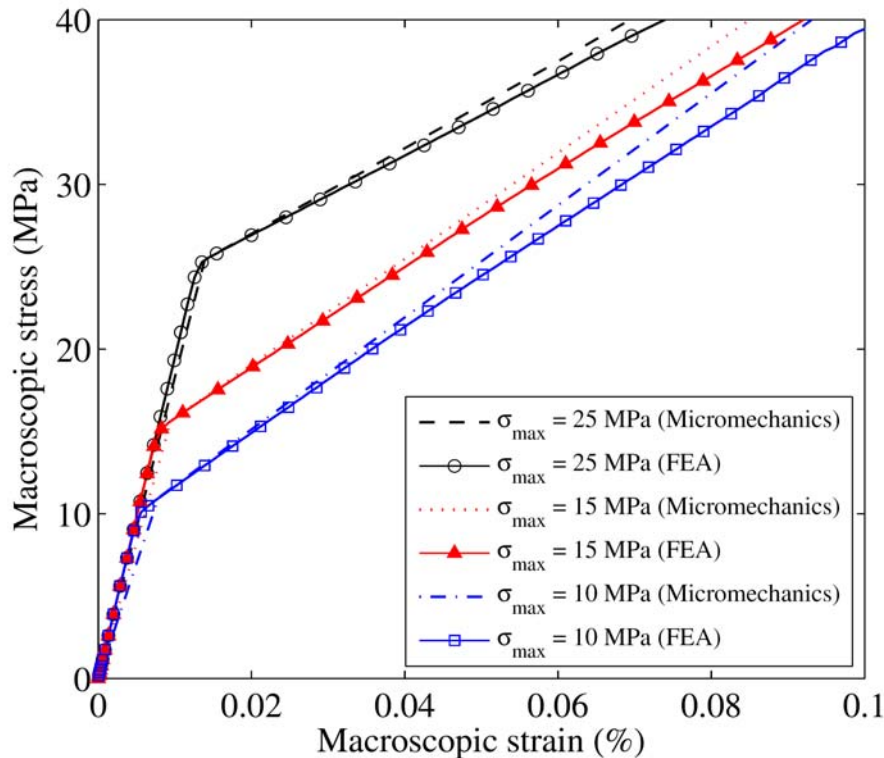


# Finite Element Mesh

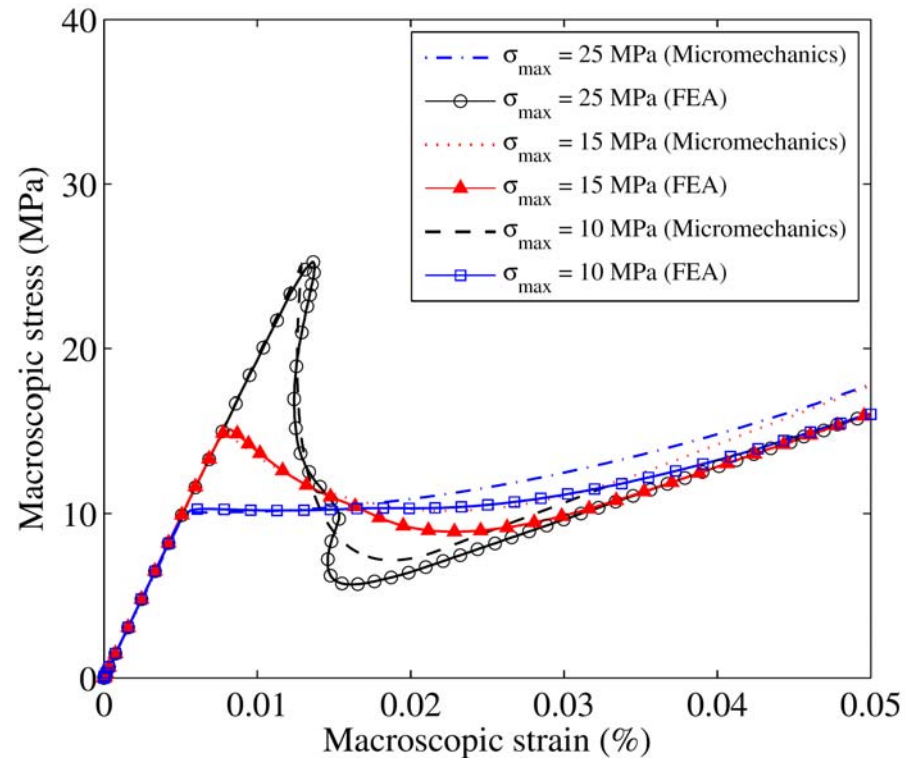


# Effect of Cohesive Strength

□ Particle size: 100  $\mu\text{m}$



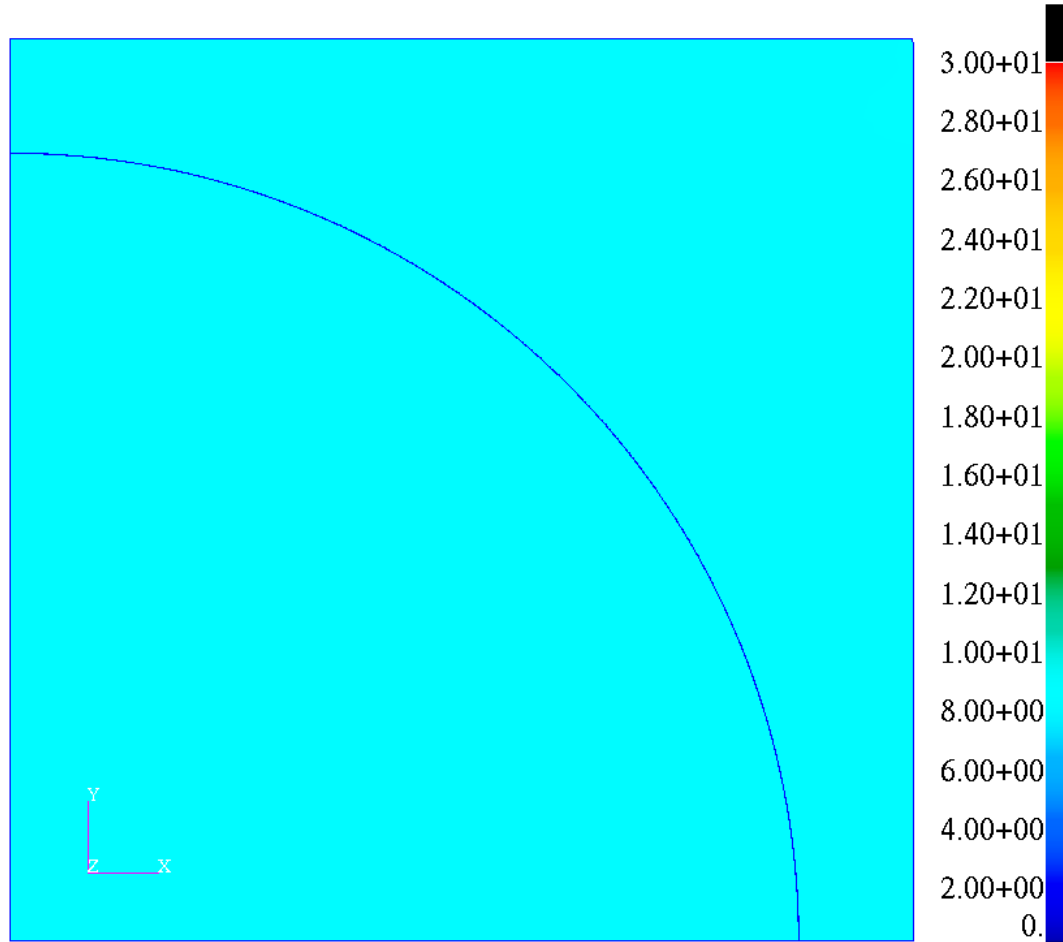
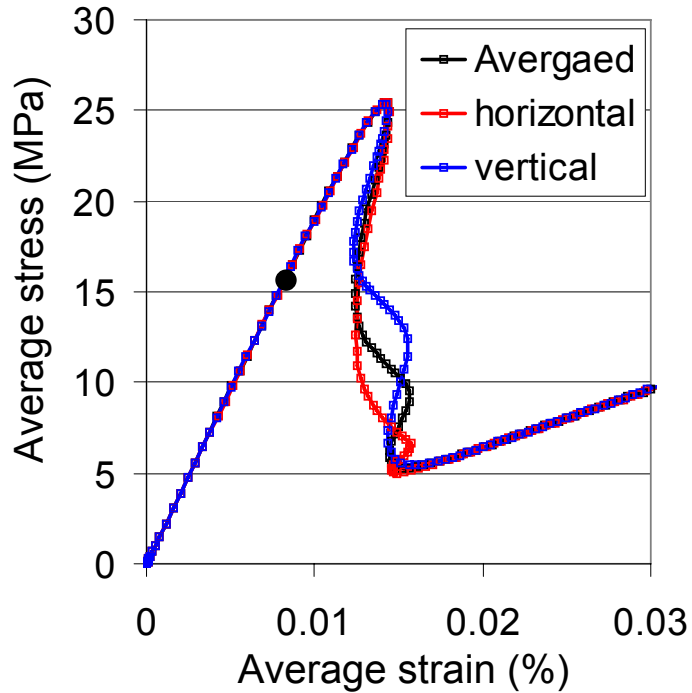
□ Particle size: 2 mm



## Micromechanics (Analytical)

D. Ngo, K. Park, G.H. Paulino, and Y. Huang, 2009, On the constitutive relation of materials with microstructure using the PPR potential-based cohesive model for interface interaction, Engineering Fracture Mechanics (submitted).

# Debonding Process 1

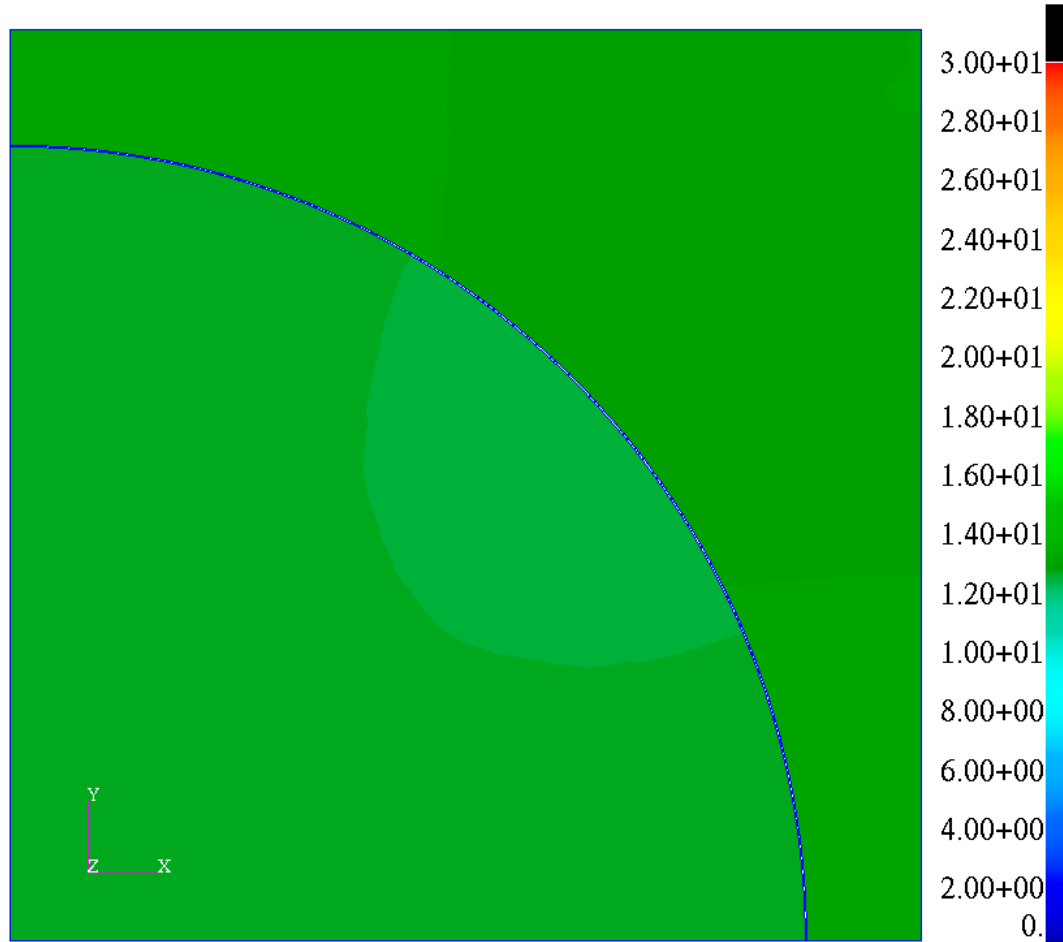
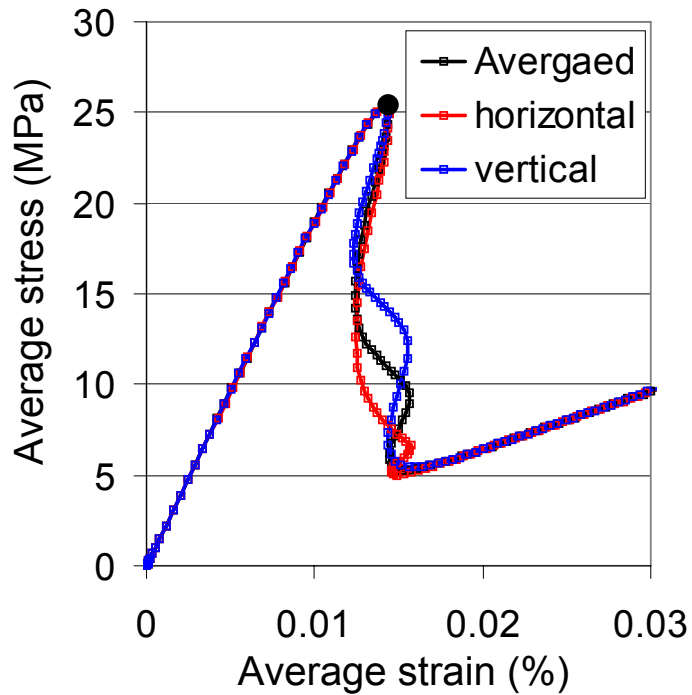


## • Fracture Parameters

G (N/m)	T <sub>max</sub> (MPa)	Shape	Slope
5	25	3	0.04



# Debonding Process 2

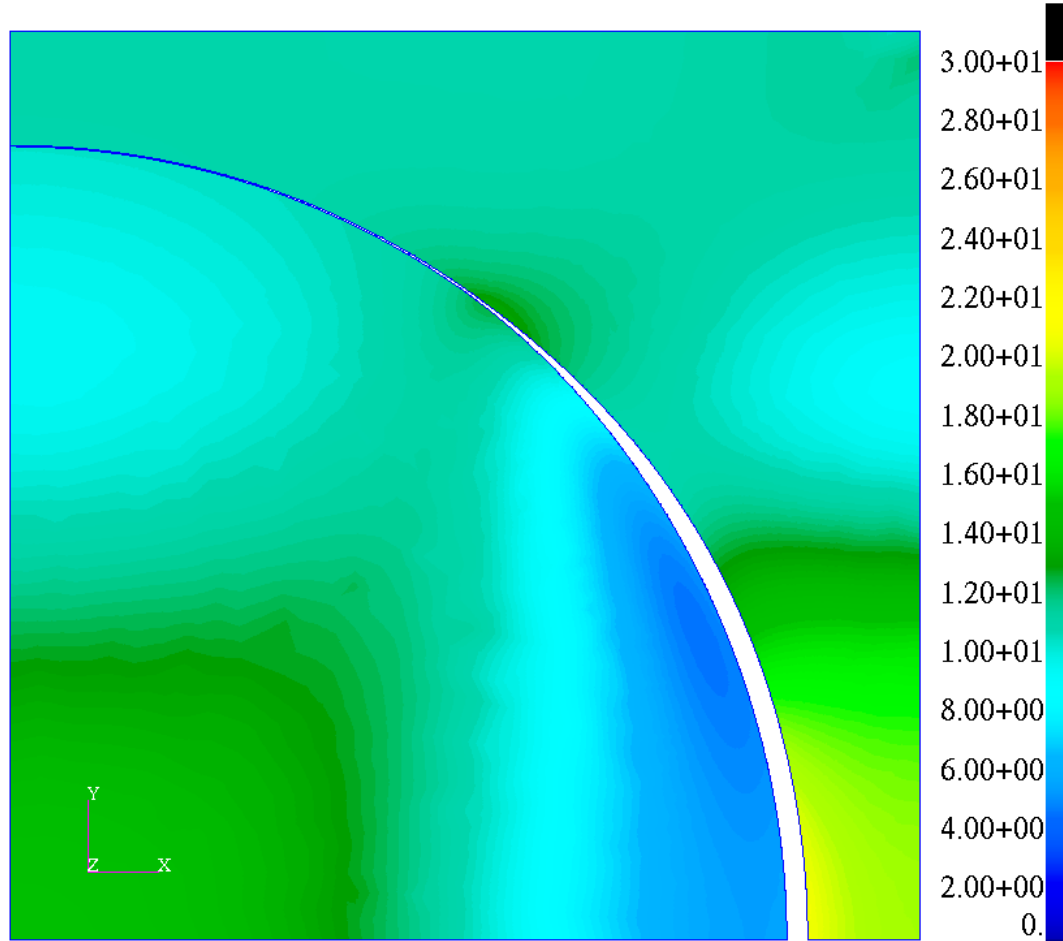
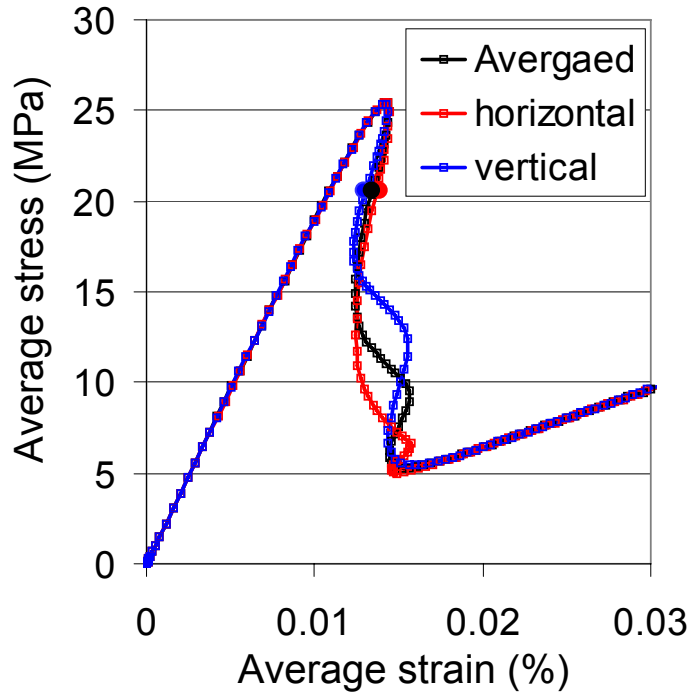


## • Fracture Parameters

G (N/m)	T <sub>max</sub> (MPa)	Shape	Slope
5	25	3	0.04



# Debonding Process 3

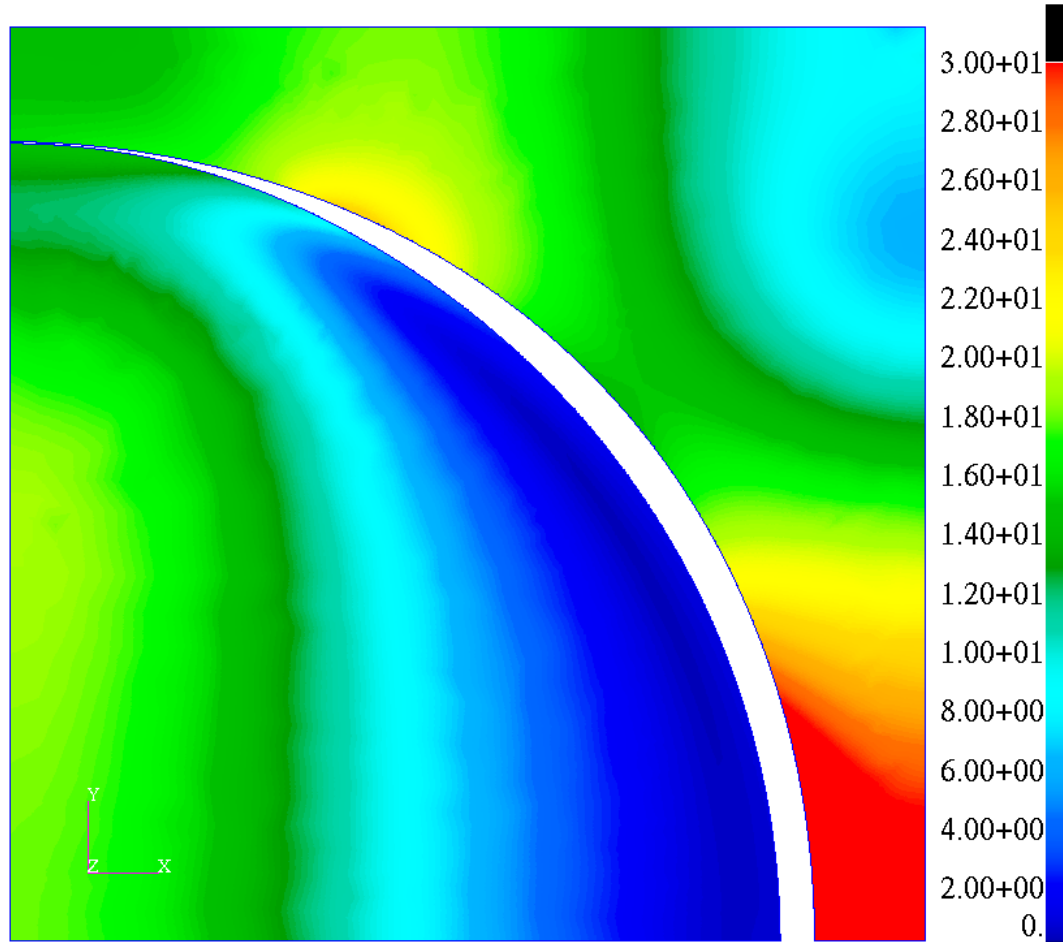
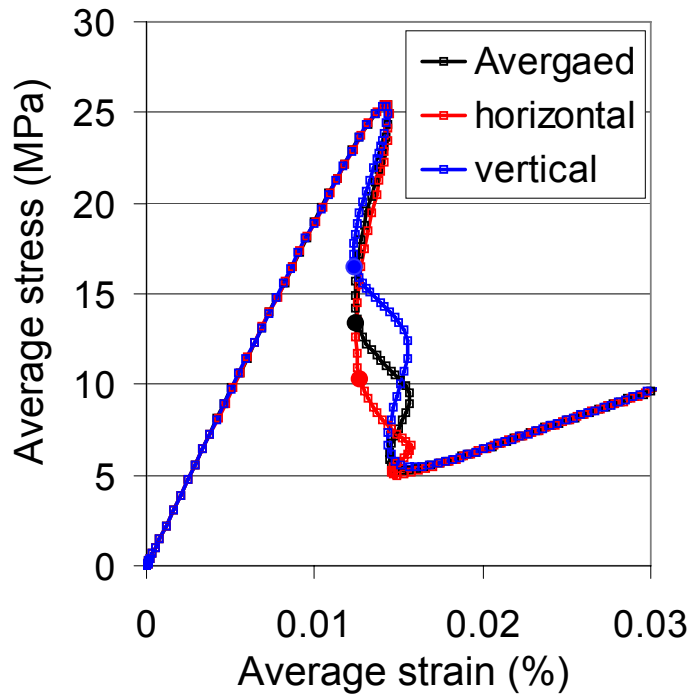


## • Fracture Parameters

G (N/m)	T <sub>max</sub> (MPa)	Shape	Slope
5	25	3	0.04



# Debonding Process 4



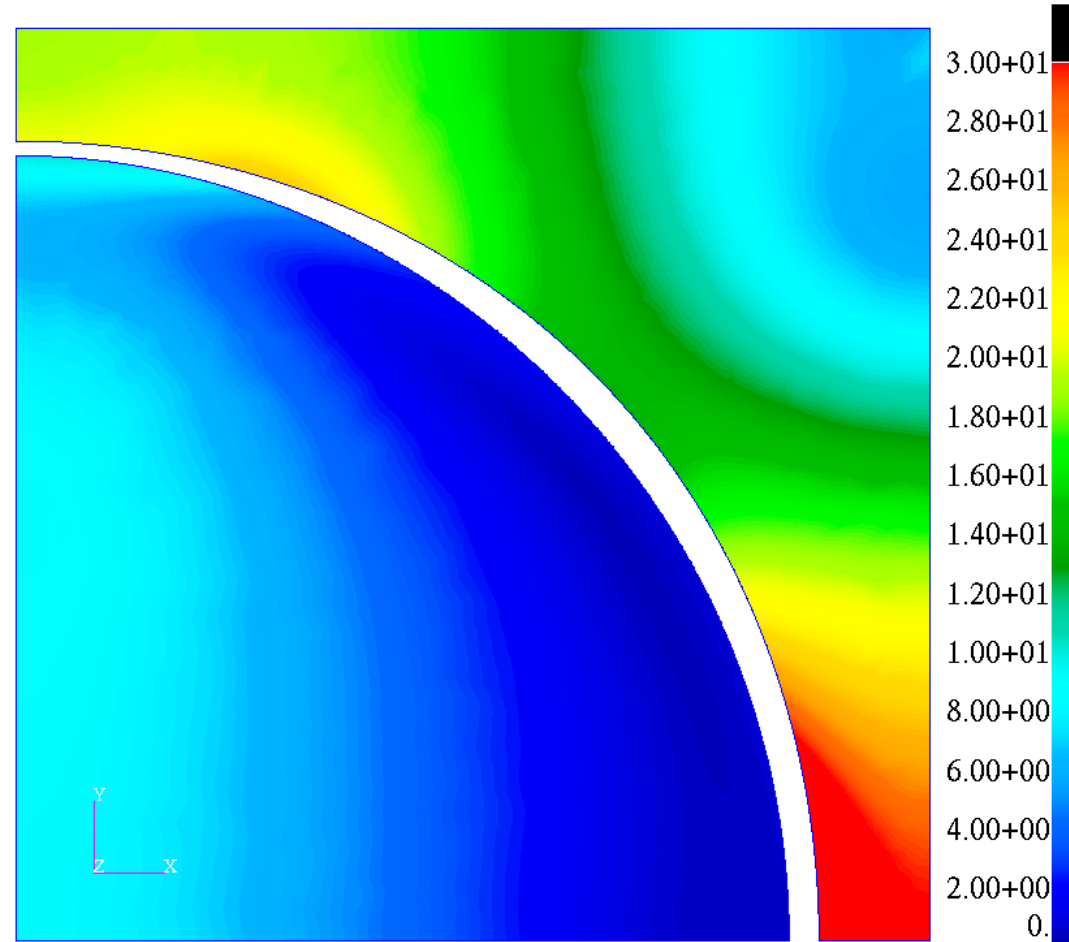
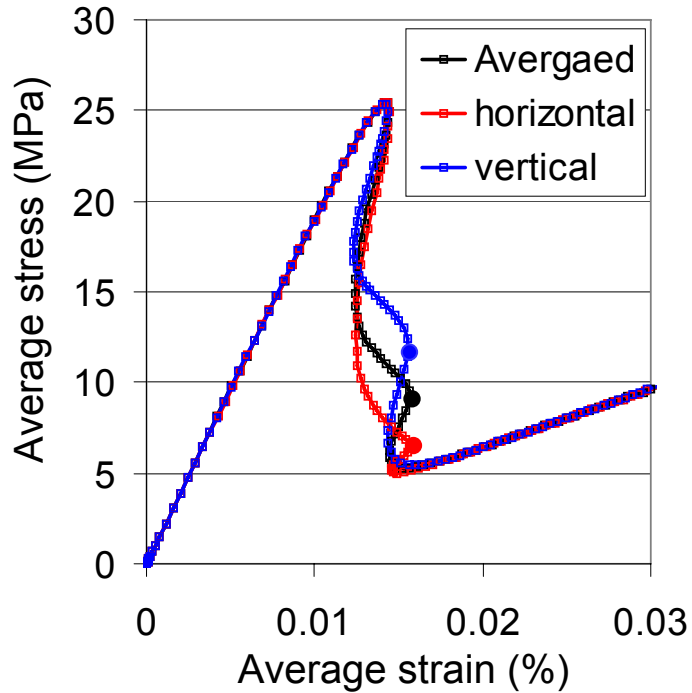
## • Fracture Parameters

G (N/m)	T <sub>max</sub> (MPa)	Shape	Slope
5	25	3	0.04





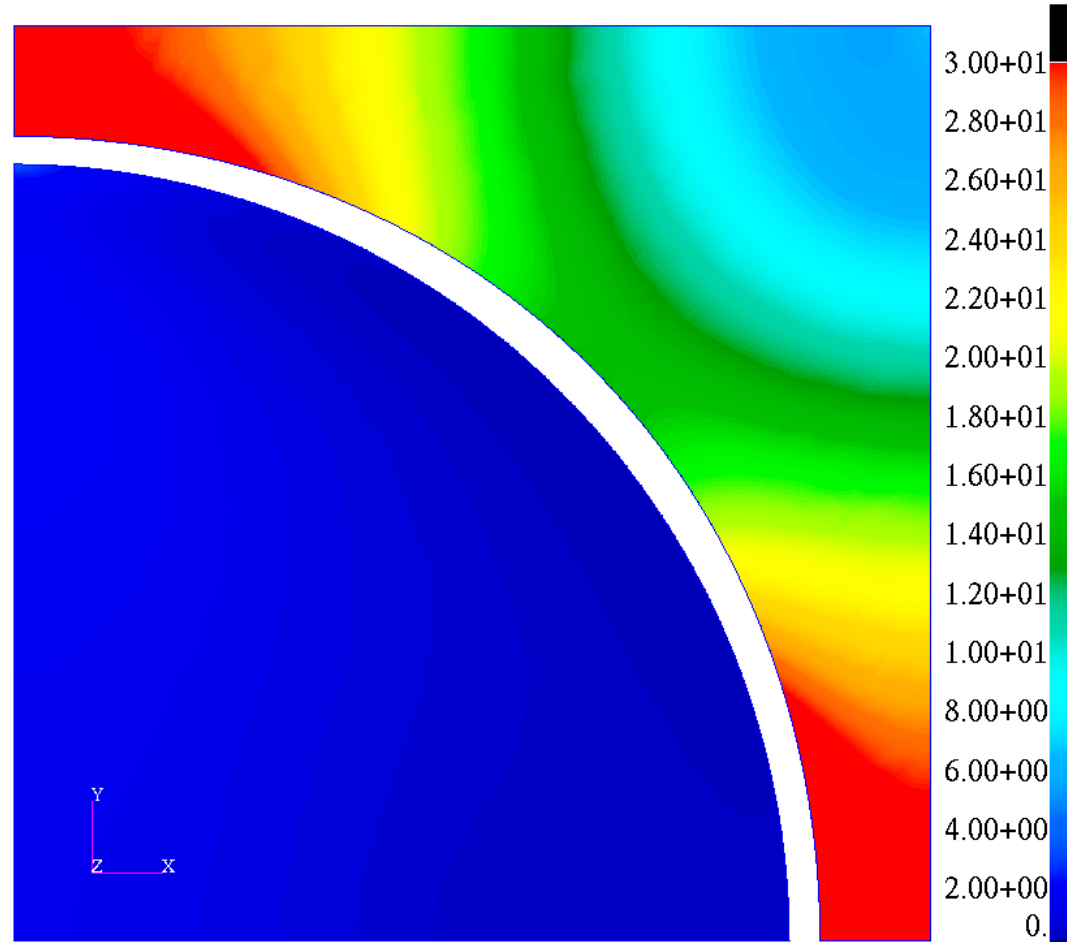
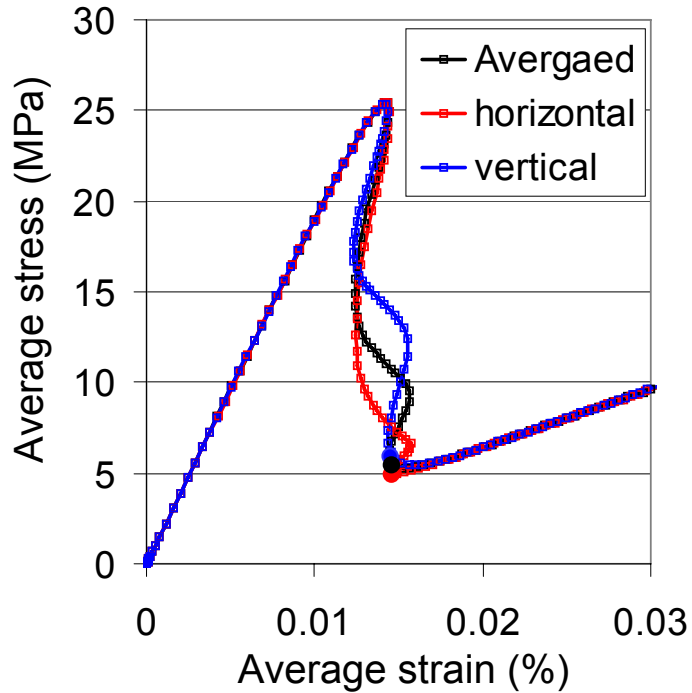
# Debonding Process 5



## • Fracture Parameters

G (N/m)	T <sub>max</sub> (MPa)	Shape	Slope
5	25	3	0.04

# Debonding Process 6

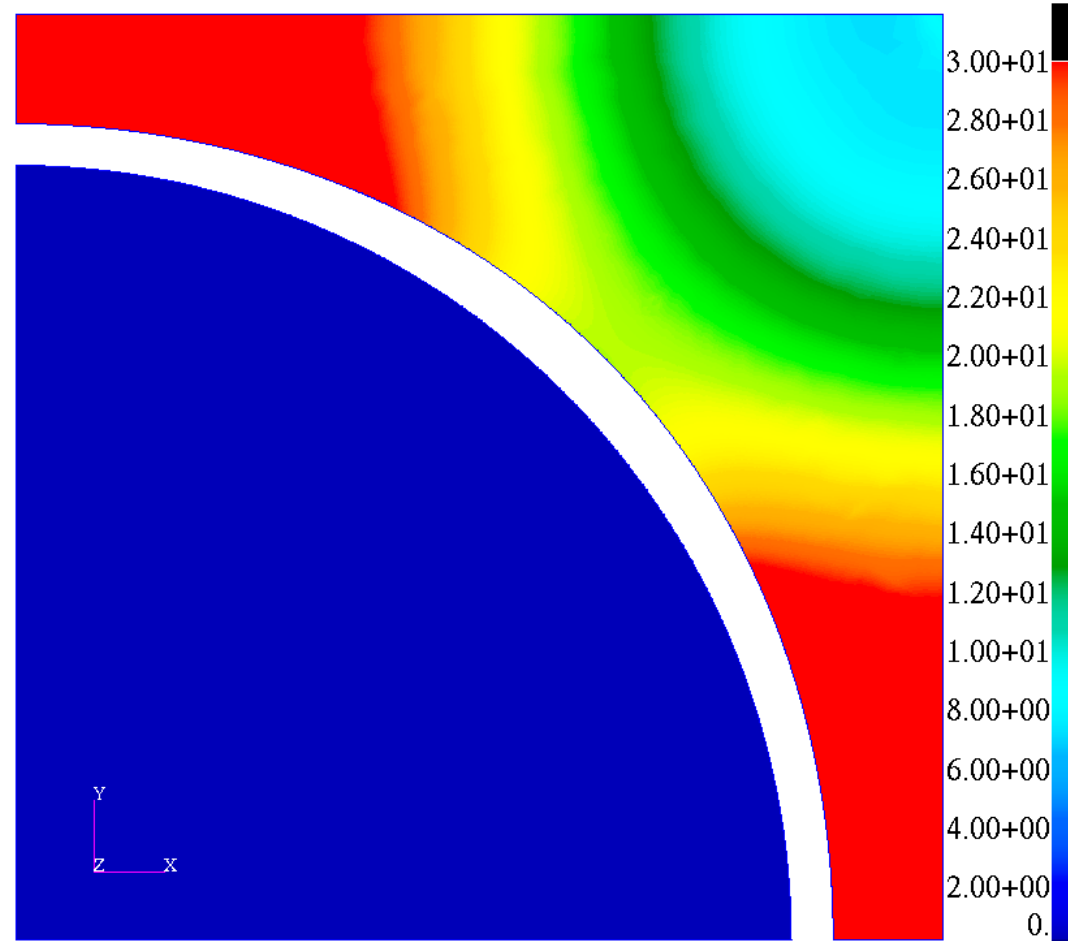
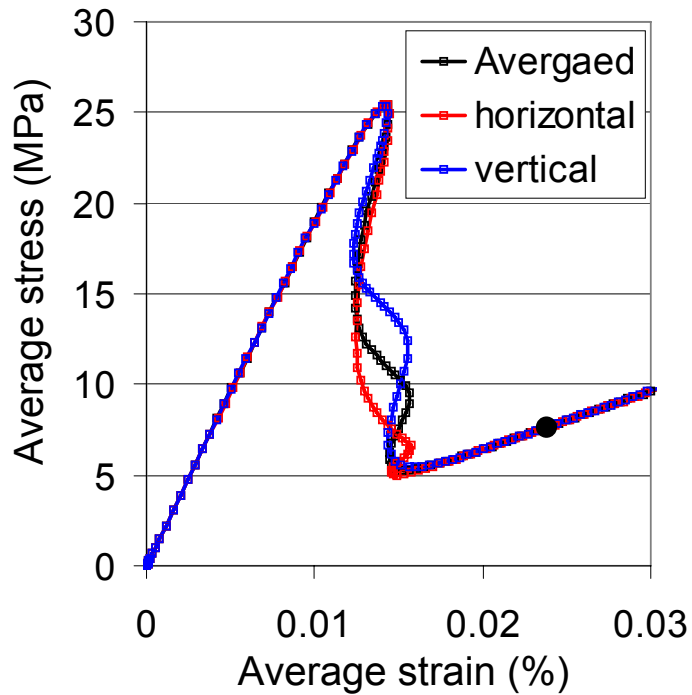


## • Fracture Parameters

G (N/m)	T <sub>max</sub> (MPa)	Shape	Slope
5	25	3	0.04



# Debonding Process 7



## • Fracture Parameters

G (N/m)	T <sub>max</sub> (MPa)	Shape	Slope
5	25	3	0.04

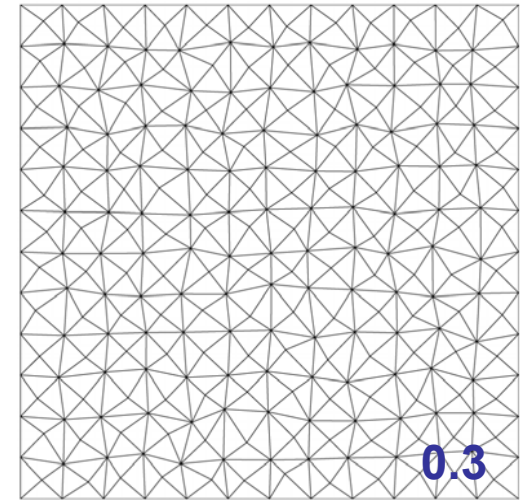
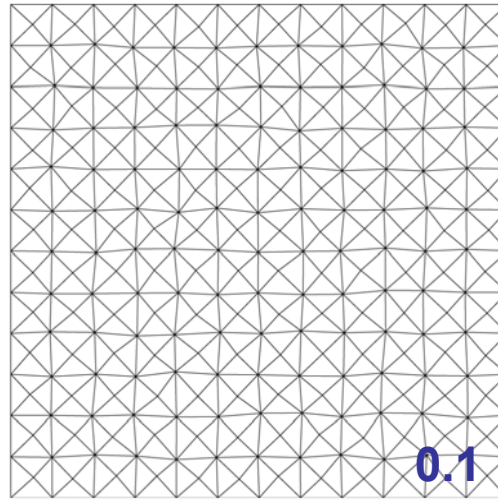
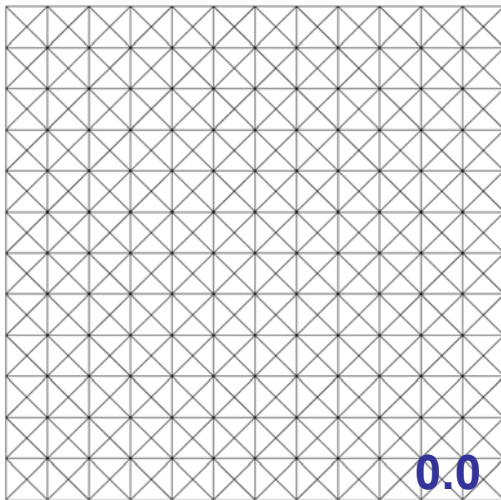
# Contents

- Introduction
- Potential-based Cohesive Model
- Quasi-Static Fracture
  - Particle/matrix debonding
- **Dynamic Fracture Problems**
  - Computational framework
  - Micro-branching and fragmentation
  - Mode I predefined crack, mixed-mode and branching
- **Virtual Internal Pair-Bond (VIPB) Model**
- **Summary**

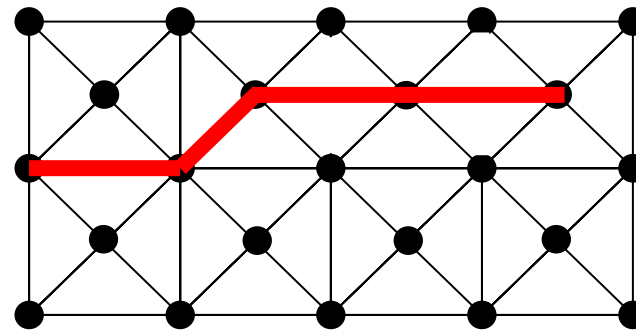
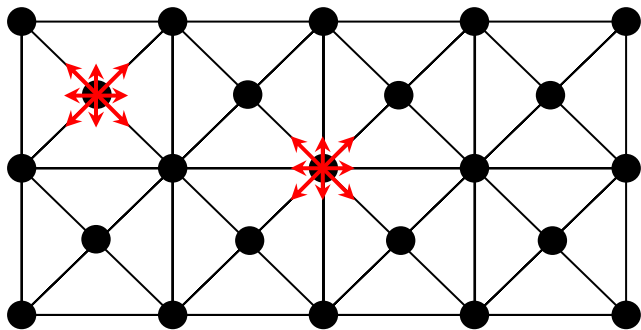


# Topological Operators

## □ Nodal Perturbation



## □ Edge-Swap



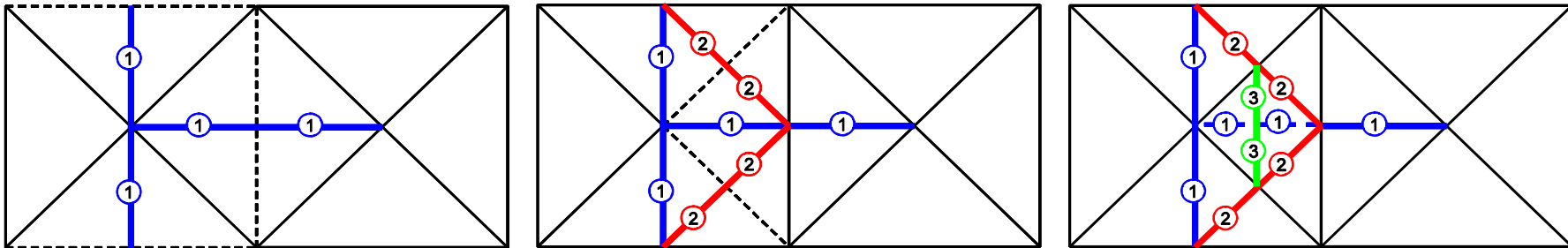
K. Park, G.H. Paulino, W. Celes, and R. Espinha, 2009, Adaptive dynamic cohesive fracture simulation using edge-swap and nodal perturbation operators, International Journal for Numerical Methods in Engineering (submitted).



# Adaptive Mesh Refinement & Coarsening

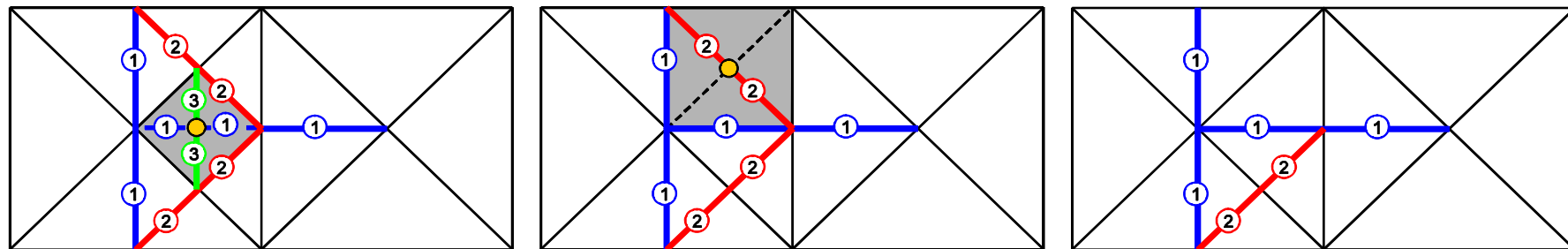
## □ Edge-Split

- Adaptive mesh refinement based on *a priori* knowledge



## □ Vertex-Removal (or Edge-Collapse)

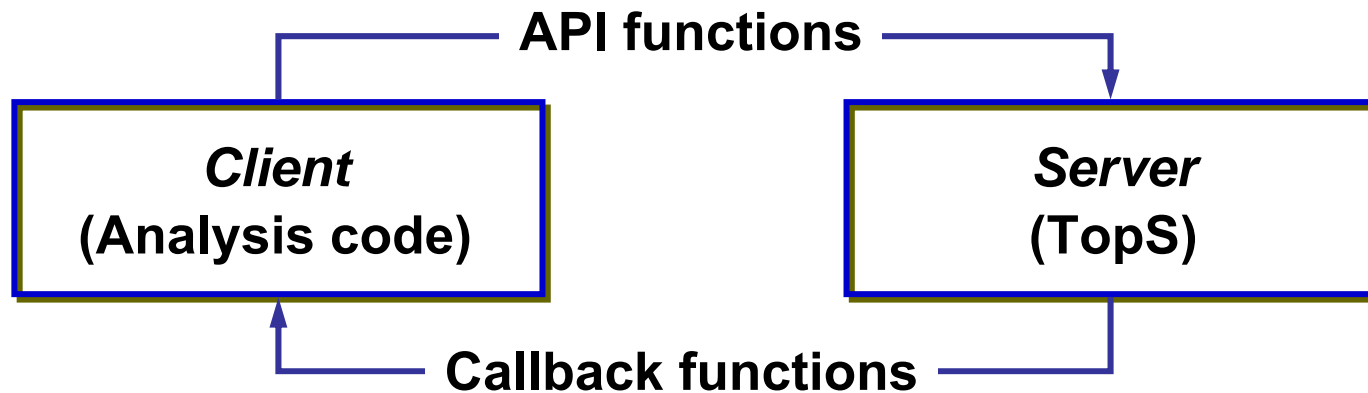
- Adaptive mesh coarsening based on *a posteriori* error estimation, i.e. root mean square of strain error



K. Park, G.H. Paulino, W. Celes, and R. Espinha, 2009, Adaptive mesh refinement and coarsening for cohesive dynamic fracture, (in preparation).

# Topology-based Data Structure (TopS)

- ❑ Complete Topological Data & Reduced Representation
- ❑ Support for Adaptive Analysis
- ❑ Client-Server Architecture
  - Separate computational mechanics from data representation



- W. Celes, G.H. Paulino, R. Espinha, 2005, A compact adjacency-based topological data structure for finite element mesh representation, IJNME 64(11), 1529-1556
- G. H. Paulino, W. Celes, R. Espinha, Z. Zhang, 2008, A general topology-based framework for adaptive insertion of cohesive elements in finite element meshes, EWC 24, 59-78
- K. Park, G.H. Paulino, W. Celes, and R. Espinha, 2009, Adaptive dynamic cohesive fracture simulation using edge-swap and nodal perturbation operators, International Journal for Numerical Methods in Engineering (submitted).



# Explicit Time Integration

**Initialization: displacement, velocity, acceleration**

**for  $n = 0$  to  $n_{\max}$  do**

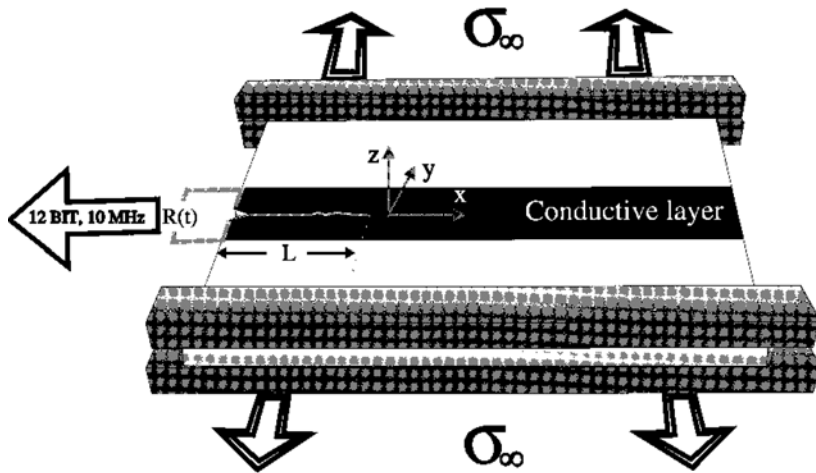
- Update displacement:  $\mathbf{u}_{n+1} = \mathbf{u}_n + \Delta t \dot{\mathbf{u}}_n + \Delta t^2 / 2 \ddot{\mathbf{u}}_n$
- Adaptive mesh coarsening (vertex-removal)
- Check the insertion of cohesive element (edge-swap)
- Update acceleration:  $\ddot{\mathbf{u}}_{n+1} = \mathbf{M}^{-1}(\mathbf{R}_{n+1}^{ext} + \mathbf{R}_{n+1}^{coh} - \mathbf{R}_{n+1}^{int})$
- Update velocity:  $\dot{\mathbf{u}}_{n+1} = \dot{\mathbf{u}}_n + \Delta t / 2 (\ddot{\mathbf{u}}_n + \ddot{\mathbf{u}}_{n+1})$
- Update boundary conditions
- Adaptive mesh refinement (edge-split, nodal perturbation)

**end**

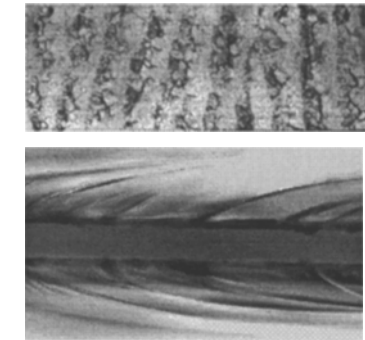
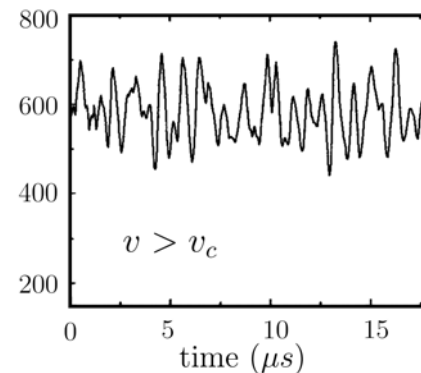
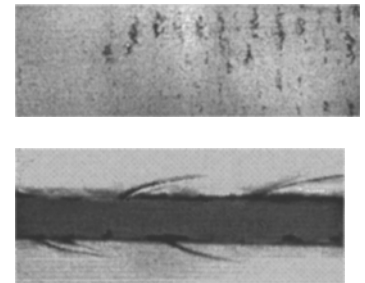
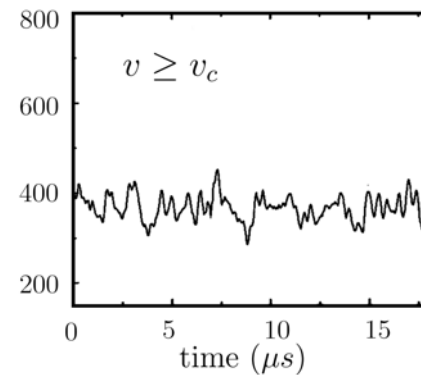
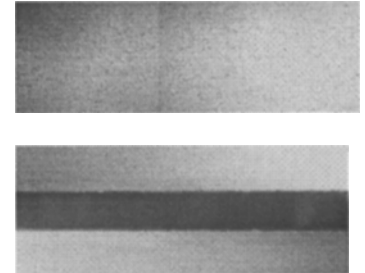
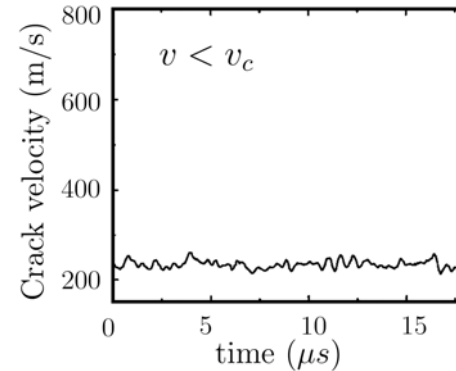
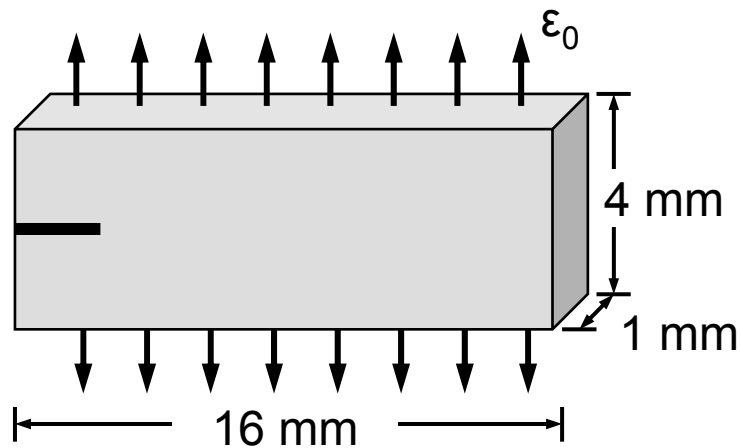




# Micro-Branching Experiment

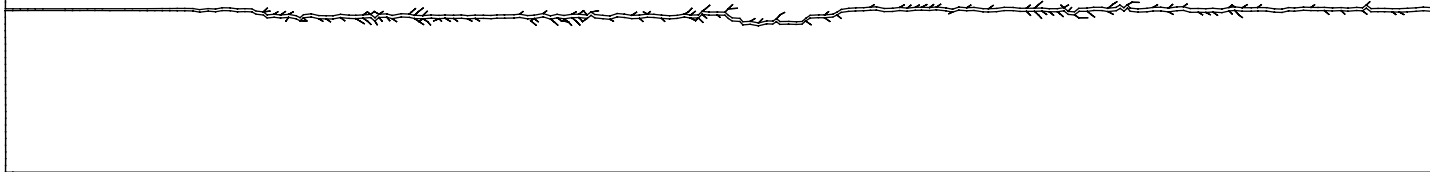


Sharon E, Fineberg J. Microbranching instability and the dynamic fracture of brittle materials. *Physical Review B* 1996; 54(10):7128–7139.

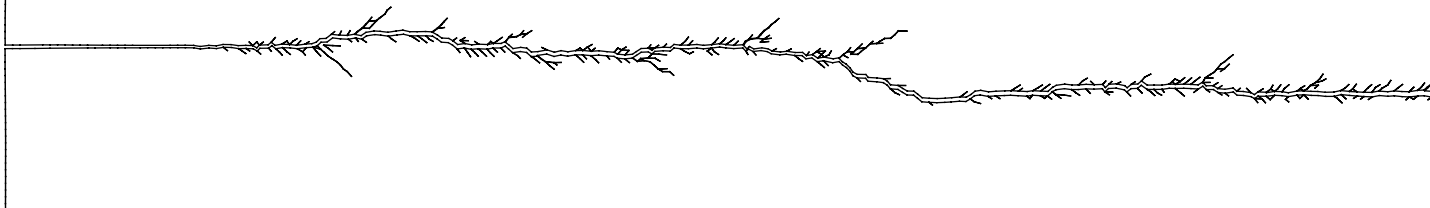


# Computational Results

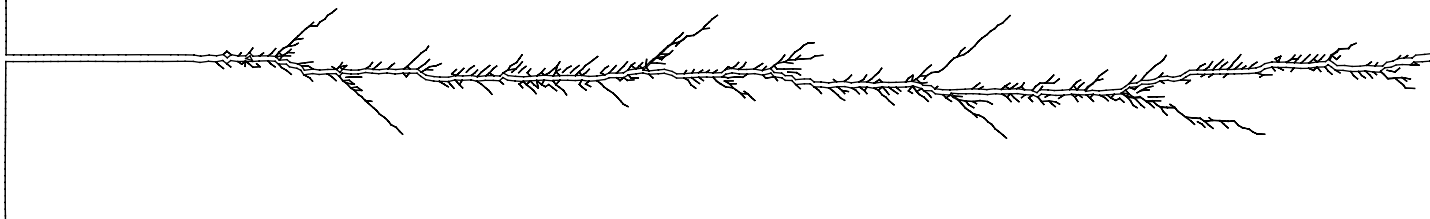
$$\varepsilon_0 = 0.010$$



$$\varepsilon_0 = 0.012$$

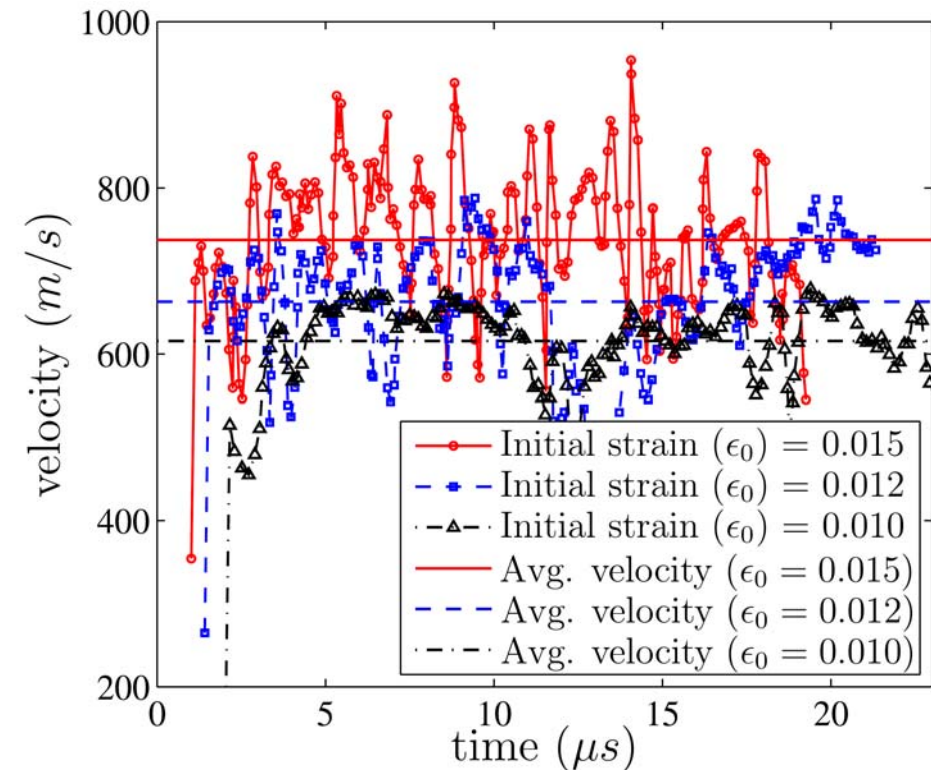


$$\varepsilon_0 = 0.015$$

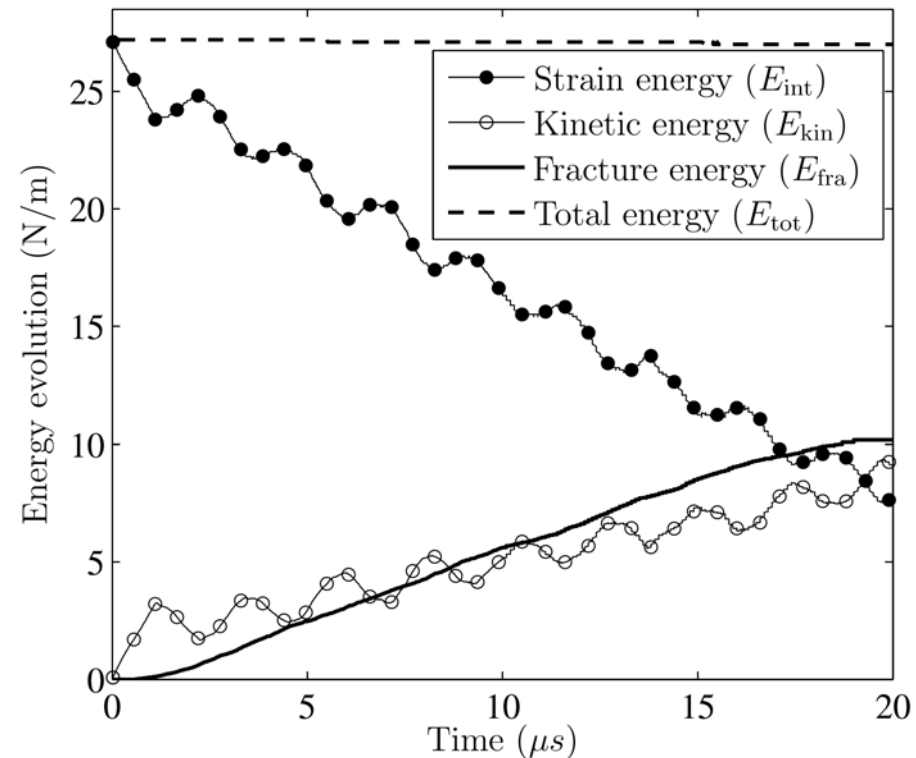


# Computational Results

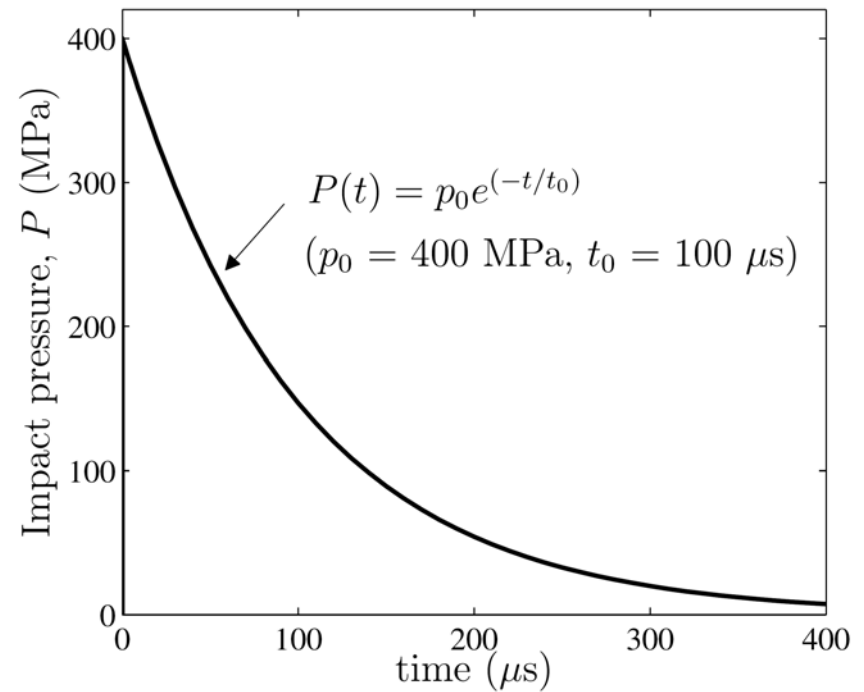
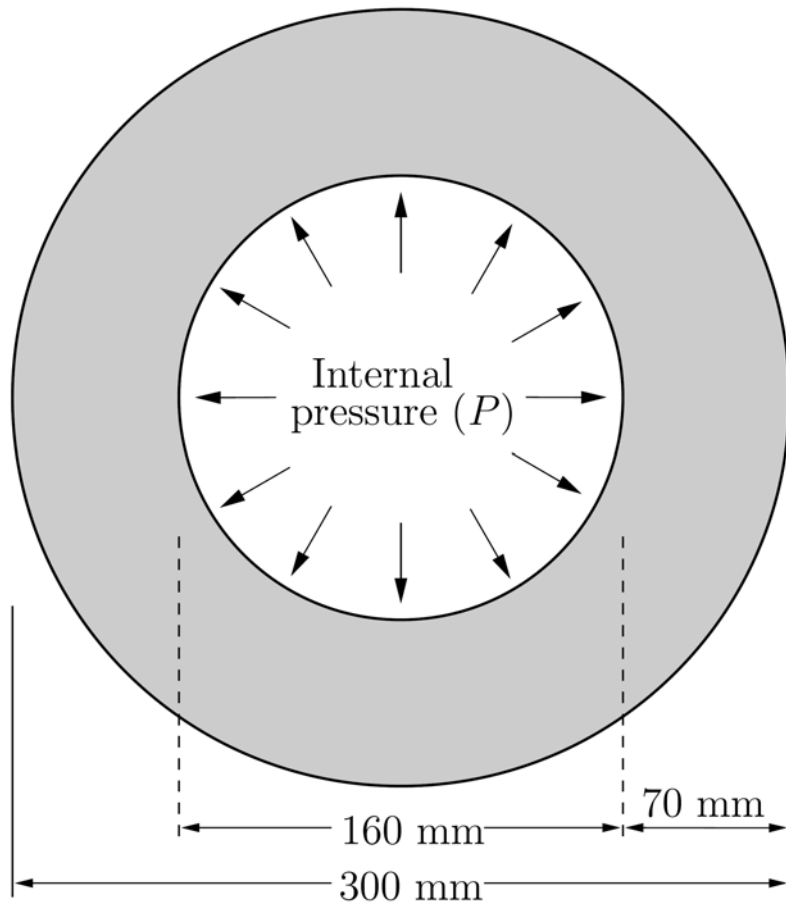
## □ Crack Velocity



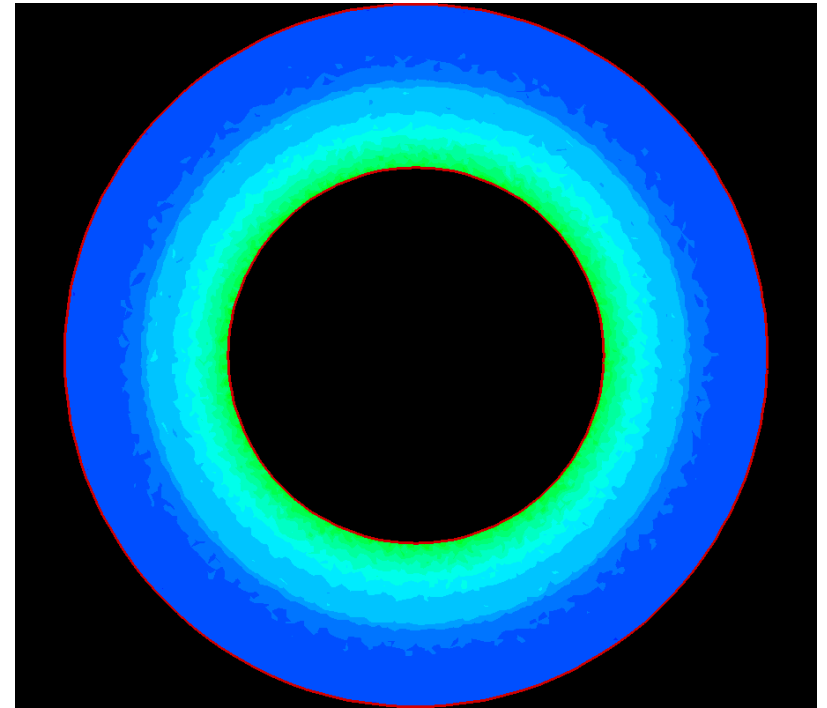
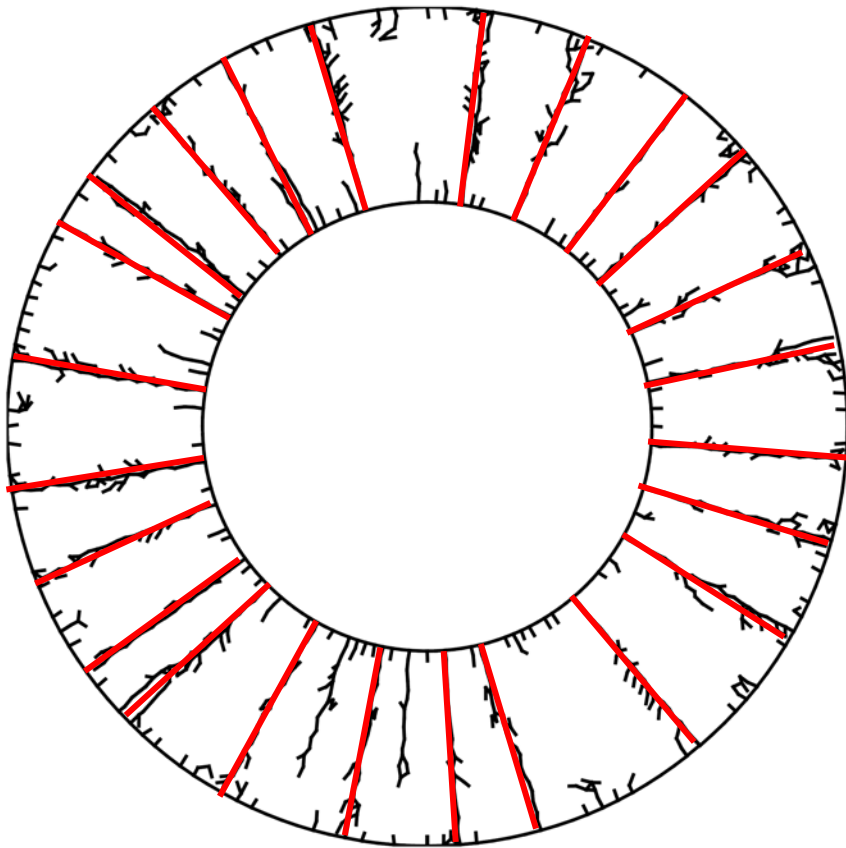
## □ Energy Evolution ( $\epsilon_0=0.015$ )



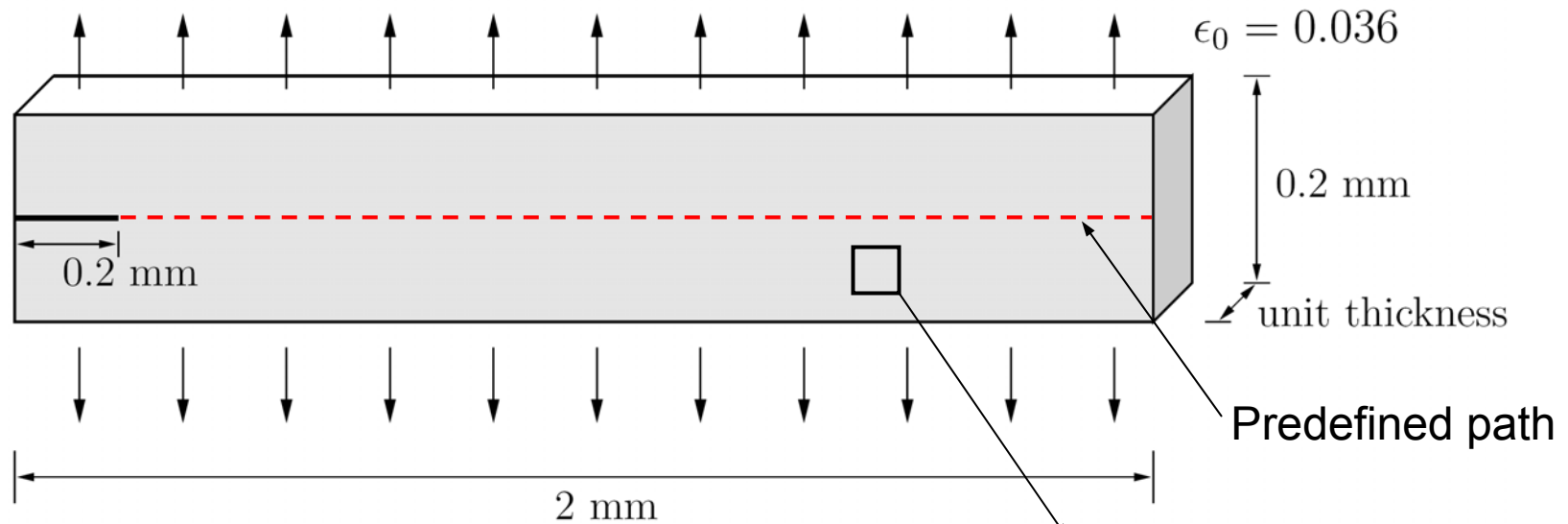
# Fragmentation Problem



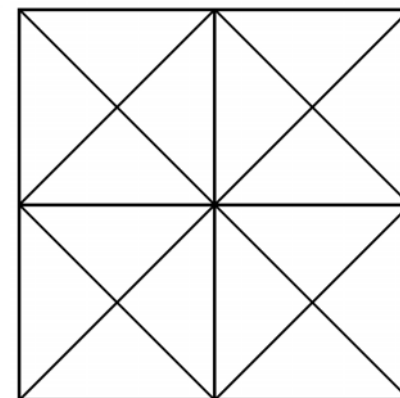
# Computational Results



# Mode I Pre-defined Crack Propagation



$E$	$\nu$	$\rho$	$G_I$	$T_{\max}$
3.24 GPa	0.35	1190 kg/m <sup>3</sup>	352 N/m	324 MPa

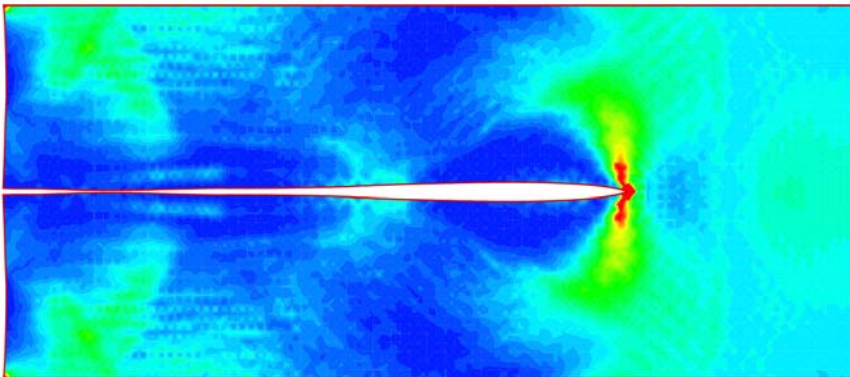
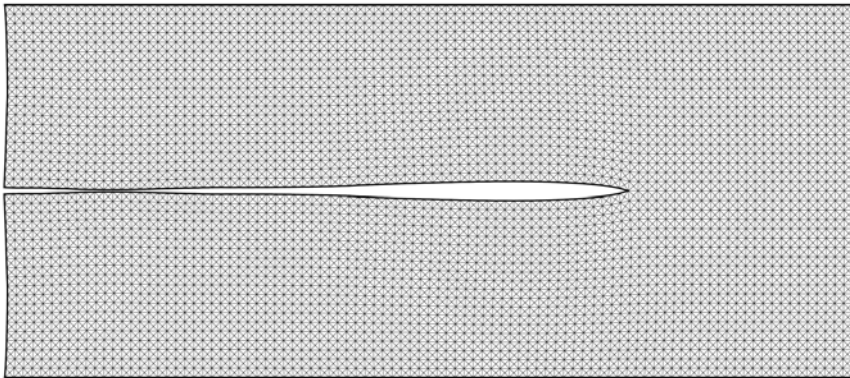


4k mesh

# Computational Results

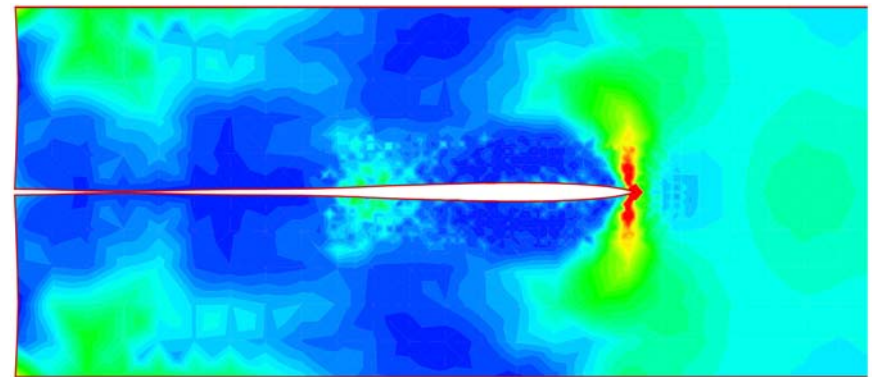
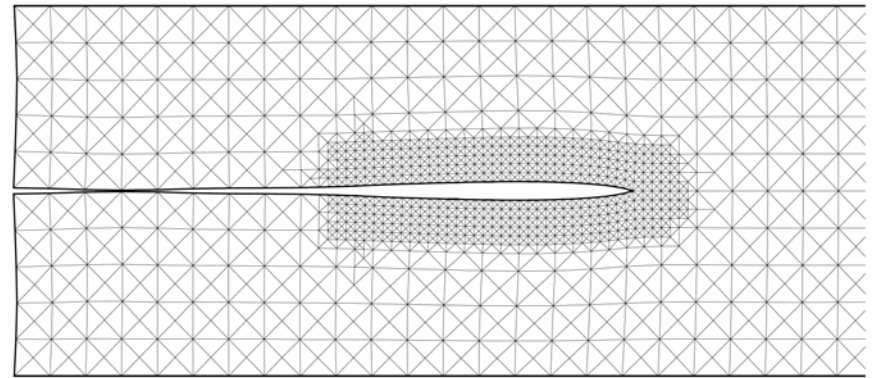
## □ Uniform Mesh Refinement

- 400x40 mesh grid
- Element size:  $5\mu\text{m}$
- 64000 elements, 128881 nodes

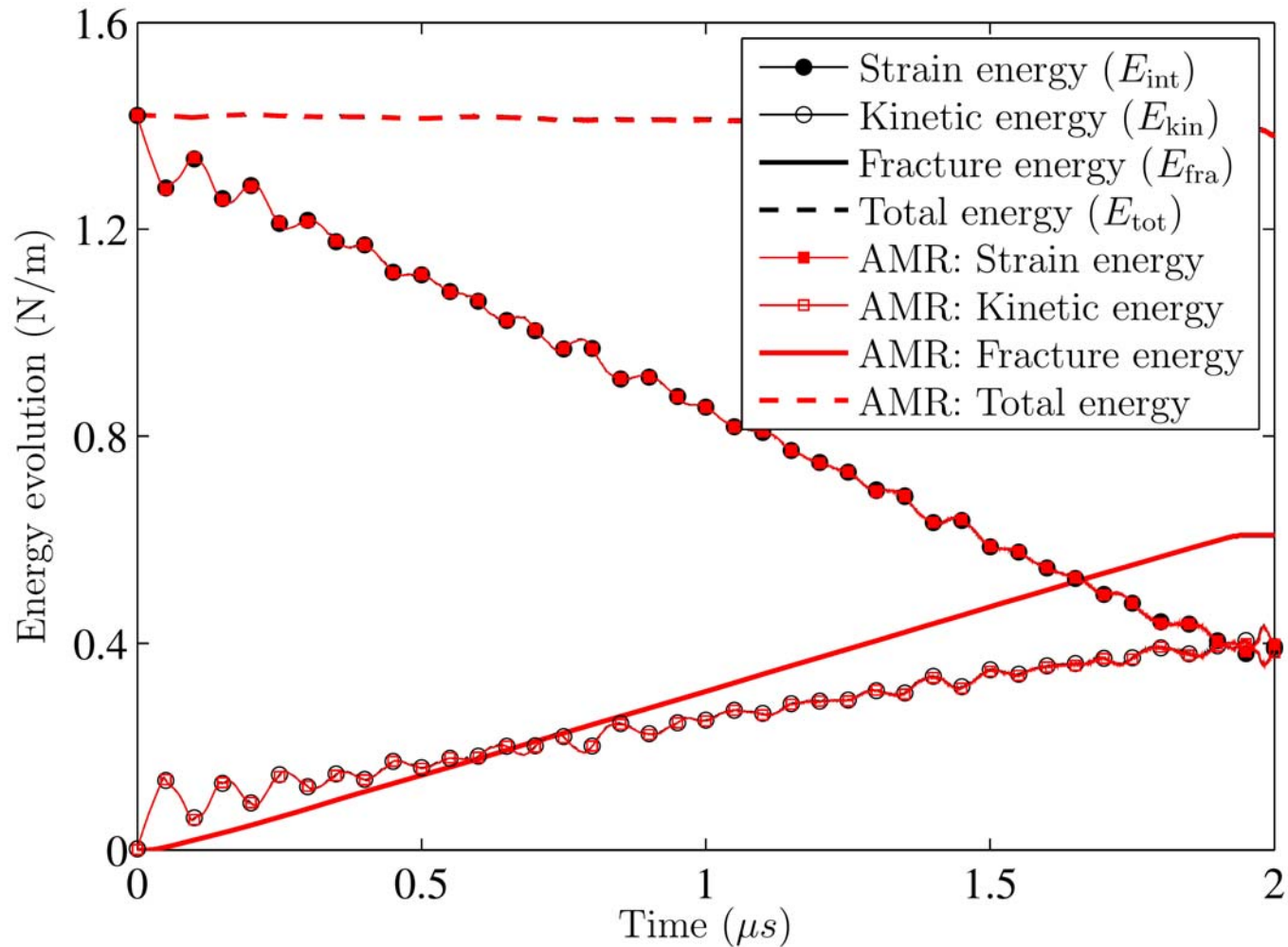


## □ Adaptive Mesh Refinement

- 100x10 mesh grid
- Element size:  $20\sim 5\mu\text{m}$
- 4448 elements, 9147 nodes

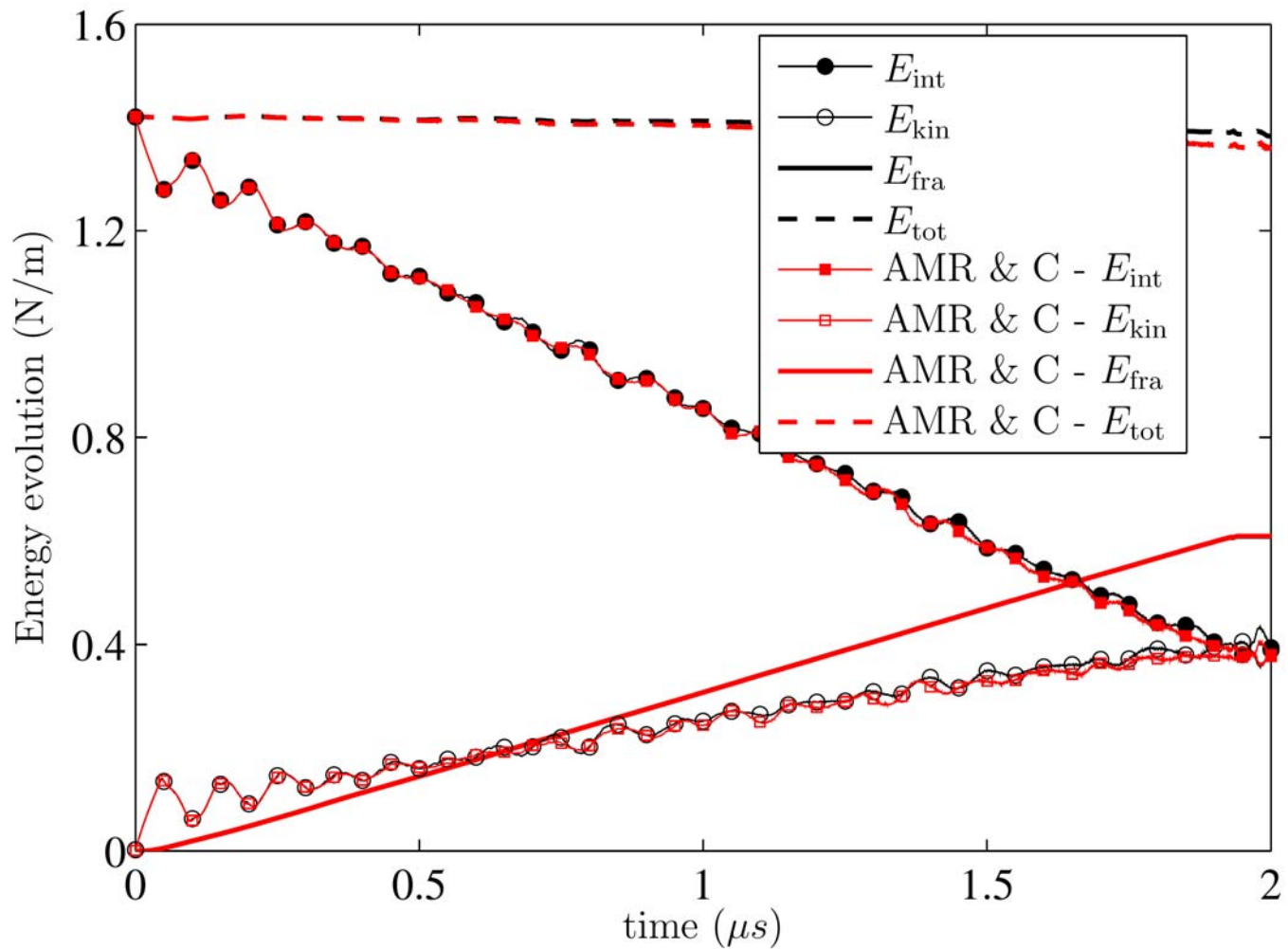


# Computational Results (AMR)



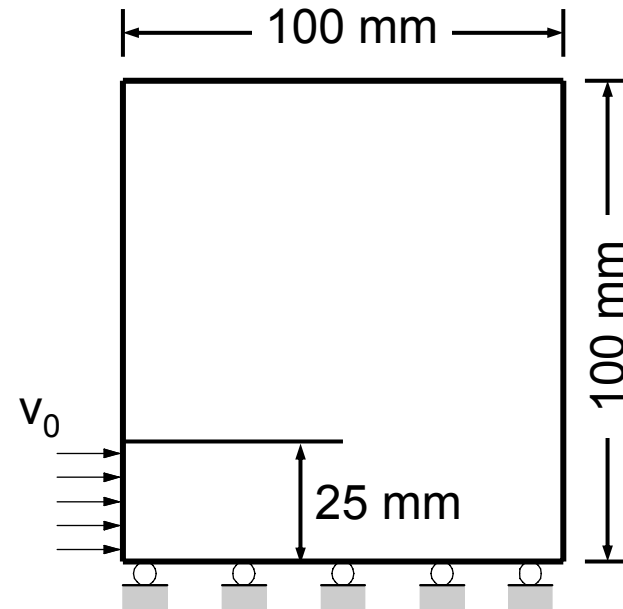
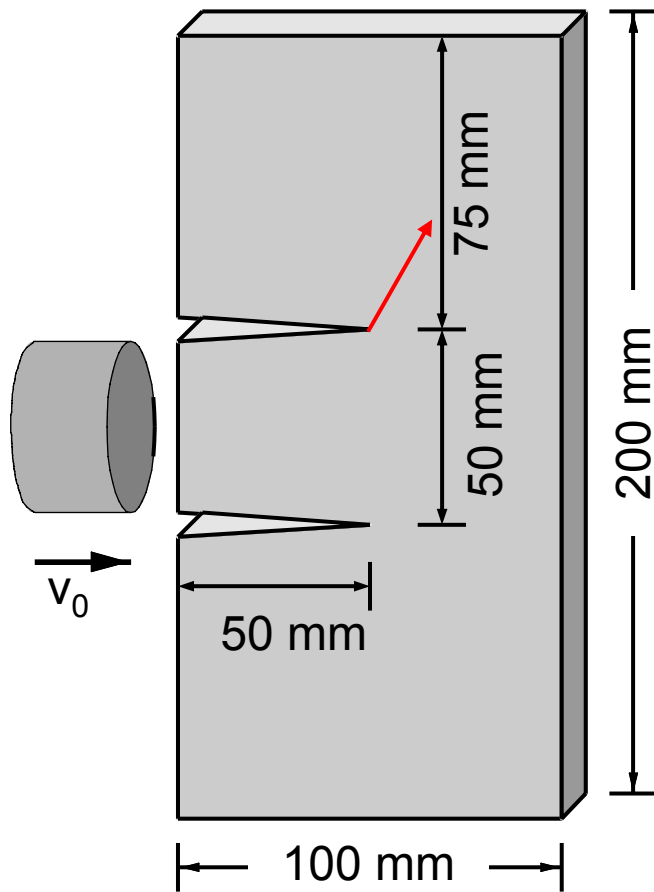


# Computational Results (AMR+C)



# Mixed-Mode Crack Propagation

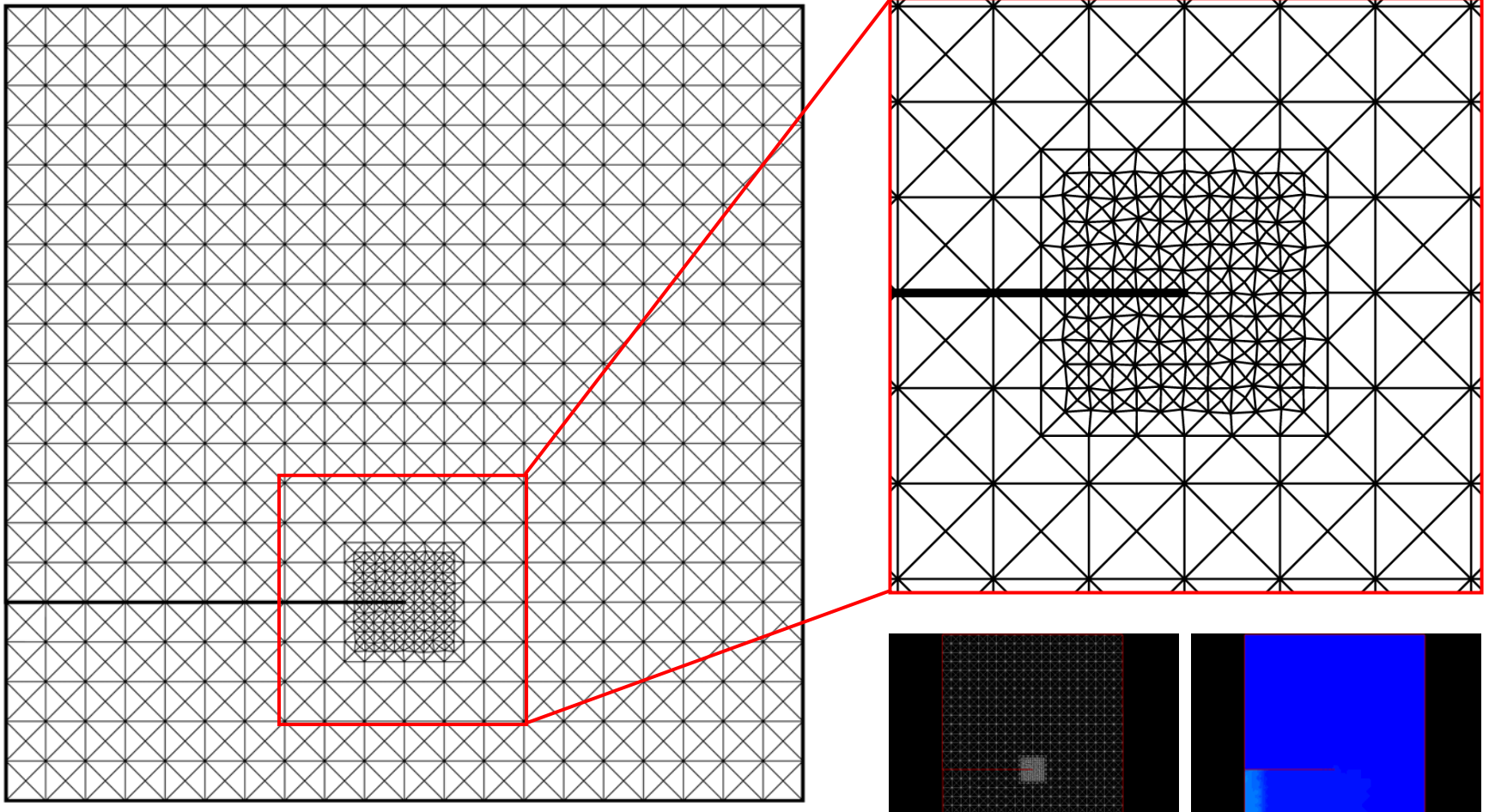
## □ Kalthoff-Winkler's Experiments



Kalthoff, J. F., Winkler, S., 1987. Failure mode transition at high rates of shear loading. International Conference on Impact Loading and Dynamic Behavior of Materials 1, 185–195.

# Finite Element Mesh

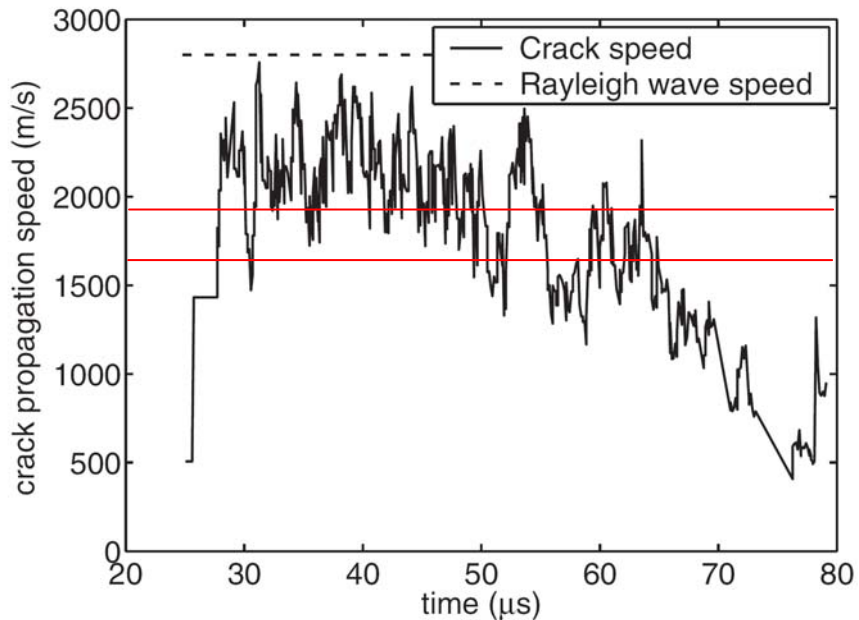
## □ Initial Discretization



Animations (FE Mesh & Strain energy)

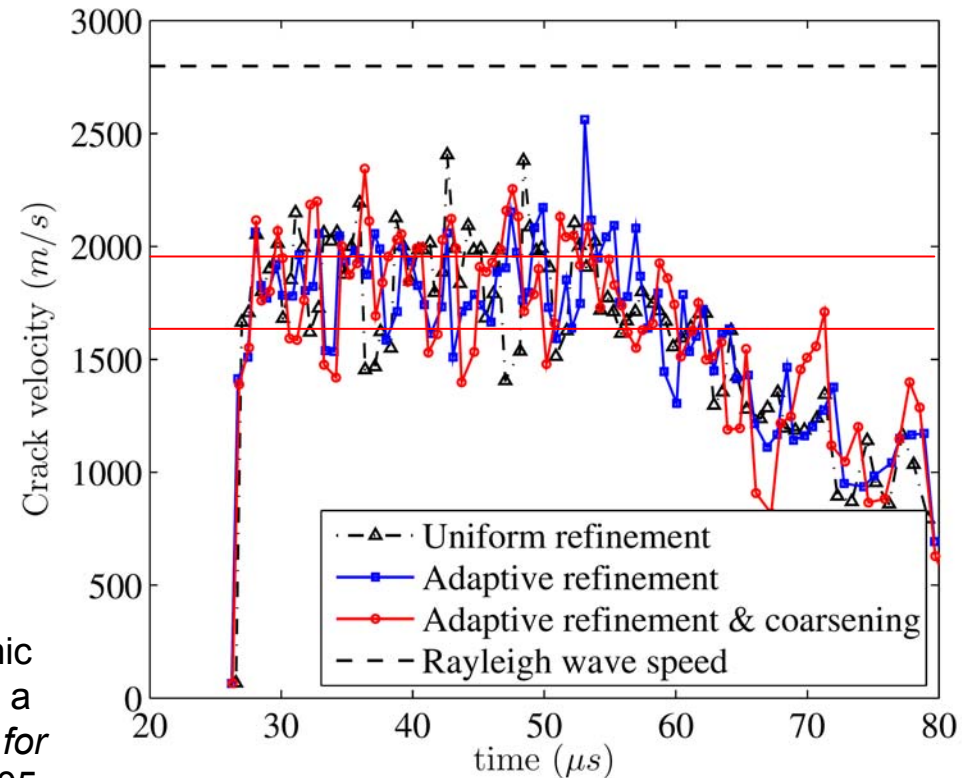
# Computational Results

## Previous results (X-FEM)

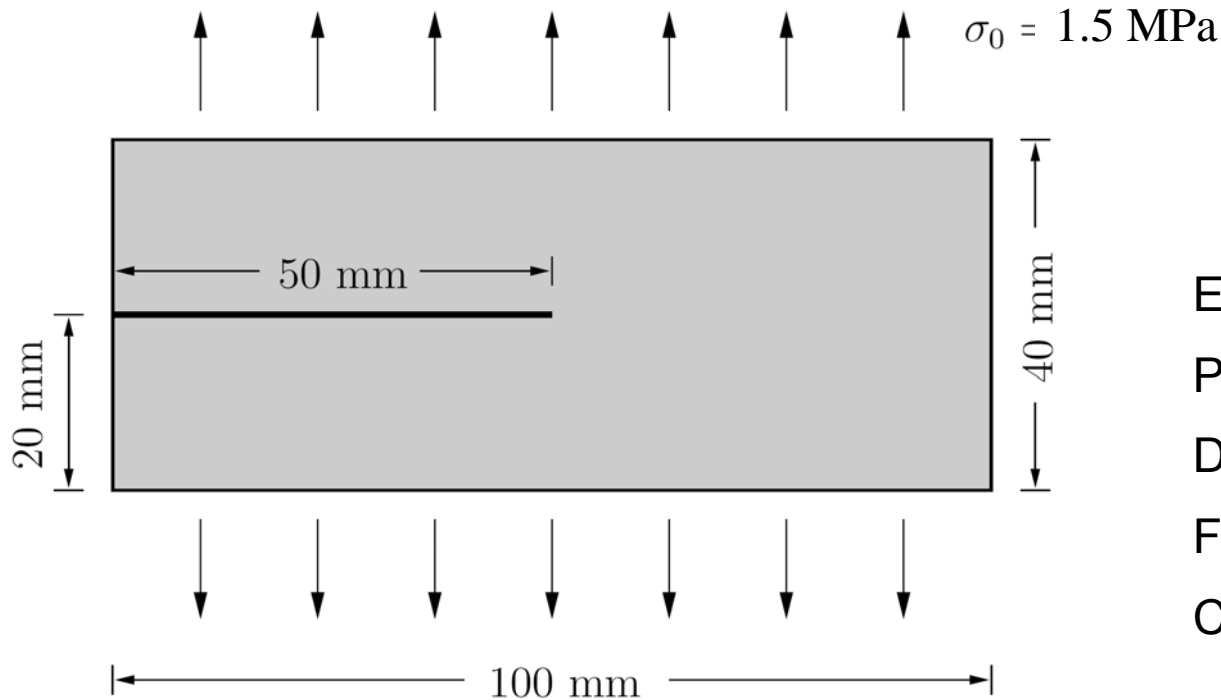


Belytschko, T., Chen, H., Xu, J., Zi, G., 2003. Dynamic crack propagation based on loss of hyperbolicity and a new discontinuous enrichment. *International Journal for Numerical Methods in Engineering* 58 (12), 1873–1905.

## □ Crack Velocity



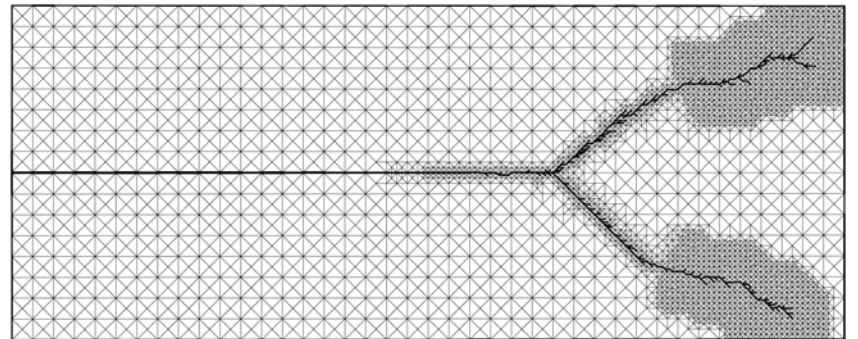
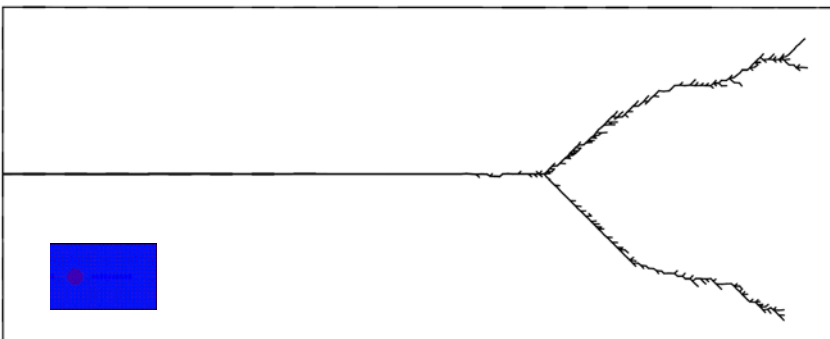
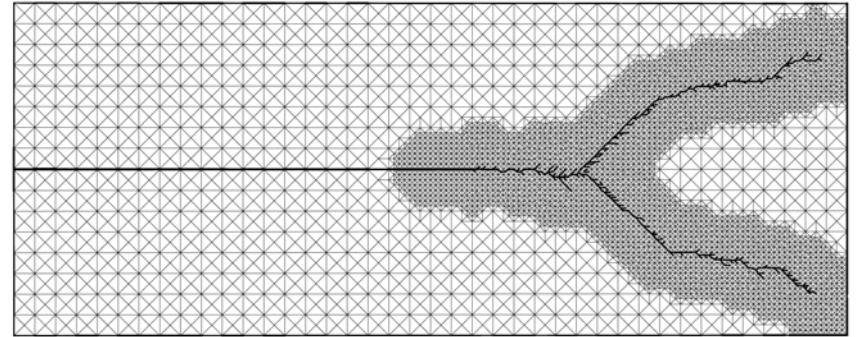
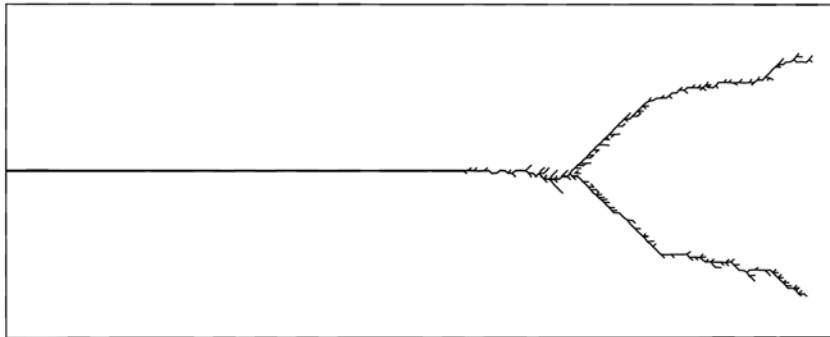
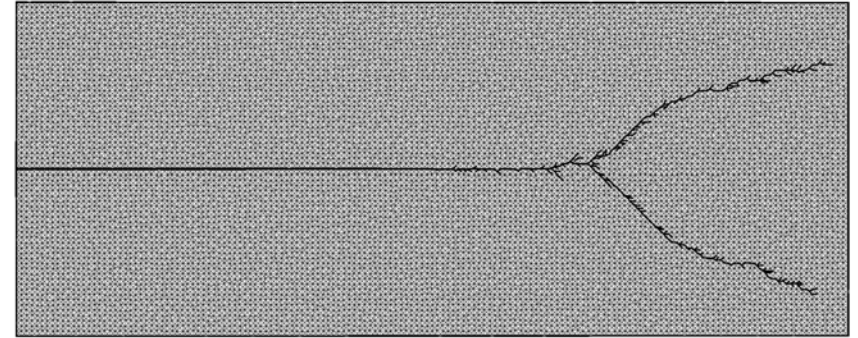
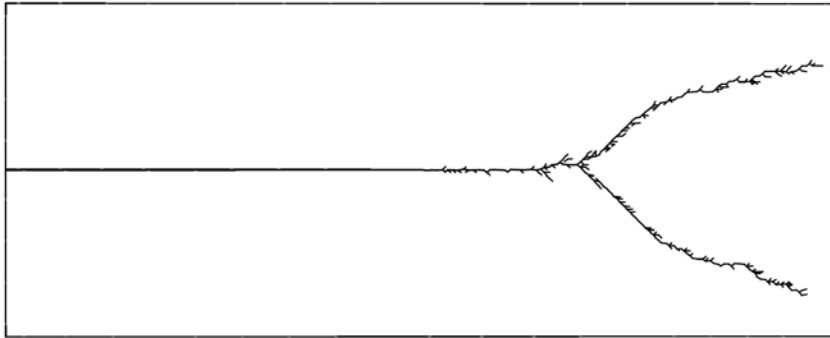
# Branching Problem



- Elastic modulus: 32GPa
- Poisson's ratio: 0.2
- Density: 2450 kg/m<sup>3</sup>
- Fracture energy: 3N/m
- Cohesive strength: 12 MPa



# Computational Results



# Contents

- Introduction
- Potential-based Cohesive Model
- Quasi-Static Fracture
  - Particle/matrix debonding
- Dynamic Fracture Problems
  - Computational framework
  - Micro-branching and fragmentation
  - Mode I predefined crack, mixed-mode and branching
- Virtual Internal Pair-Bond (VIPB) Model
- Summary



# Summary

- **The potential-based constitutive model**
  - Consistent boundary conditions
  - Physical fracture parameters
  
- **Adaptive operators**
  - Insertion of cohesive elements (Extrinsic model)
  - Nodal perturbation, Edge-swap
  - Edge-split, Vertex-removal
  
- **Effective and efficient computational framework to simulate physical phenomena associated with quasi-static fracture, dynamic fracture, branching, and fragmentation problems**





# Contributions

- K. Park, G.H. Paulino, and J.R. Roesler, 2009, A unified potential-based cohesive model of mixed-mode fracture, *Journal of the Mechanics and Physics of Solids* 57 (6), 891-908.
- D. Ngo, K. Park, G.H. Paulino, and Y. Huang, 2009, On the constitutive relation of materials with microstructure using the PPR potential-based cohesive model for interface interaction, *Engineering Fracture Mechanics* (submitted).
- K. Park, G.H. Paulino, W. Celes, and R. Espinha, 2009, Adaptive dynamic cohesive fracture simulation using edge-swap and nodal perturbation operators, *International Journal for Numerical Methods in Engineering* (submitted).
- K. Park, G.H. Paulino, W. Celes, and R. Espinha, 2009, Adaptive mesh refinement and coarsening for cohesive dynamic fracture, (in preparation).
- K. Park, G.H. Paulino, and J.R. Roesler, 2008, Virtual internal pair-bond model for quasi-brittle materials, *Journal of Engineering Mechanics-ASCE* 134 (10), 856-866.
- K. Park, J.P. Pereira, C.A. Duarte, and G.H. Paulino, 2009, Integration of singular enrichment functions in the generalized/extended finite element method for three-dimensional problems, *International Journal for Numerical Methods in Engineering* 78 (10), 1220-1257.
- K. Park, G.H. Paulino, and J.R. Roesler, 2008, Determination of the kink point in the bilinear softening model for concrete, *Engineering Fracture Mechanics* 75 (13), 3806-3818.
- J.R. Roesler, G.H. Paulino, K. Park, and C. Gaedicke, 2007, Concrete fracture prediction using bilinear softening, *Cement & Concrete Composites* 29 (4), 300-312.
- J.R. Roesler, G.H. Paulino, C. Gaedicke, A. Bordelon, and K. Park, 2007, Fracture behavior of functionally graded concrete materials (FGCM) for rigid pavements, *Transportation Research Record* 2037, 40-49.
- K. Park, G.H. Paulino, and J.R. Roesler, 2009, Cohesive fracture modeling of functionally graded fiber reinforced concrete composite, *ACI Materials Journal* (submitted).



# Acknowledgements

## □ **Advisor/Co-advisor**

- Glaucio H. Paulino / Jeffery R. Roesler

## □ **Committee**

- Glaucio H. Paulino, Jeffery R. Roesler, Yonggang Huang, C. Armando Duarte, Robert B. Haber, Karel Matous, Spandan Maiti, Waldemar Celes

## □ **Micromechanics**

- Yonggang Huang, Duc Ngo

## □ **Topological Data Structure**

- Waldemar Celes, Rodrigo Espinha

## □ **Fanatical Support**

- National Science Foundation (NSF)
- Federal aviation of administration (FAA)

## □ **Former/present group members and colleagues**

## □ **Special thanks to Younhee Ko**



**Thank you for your attention !**

